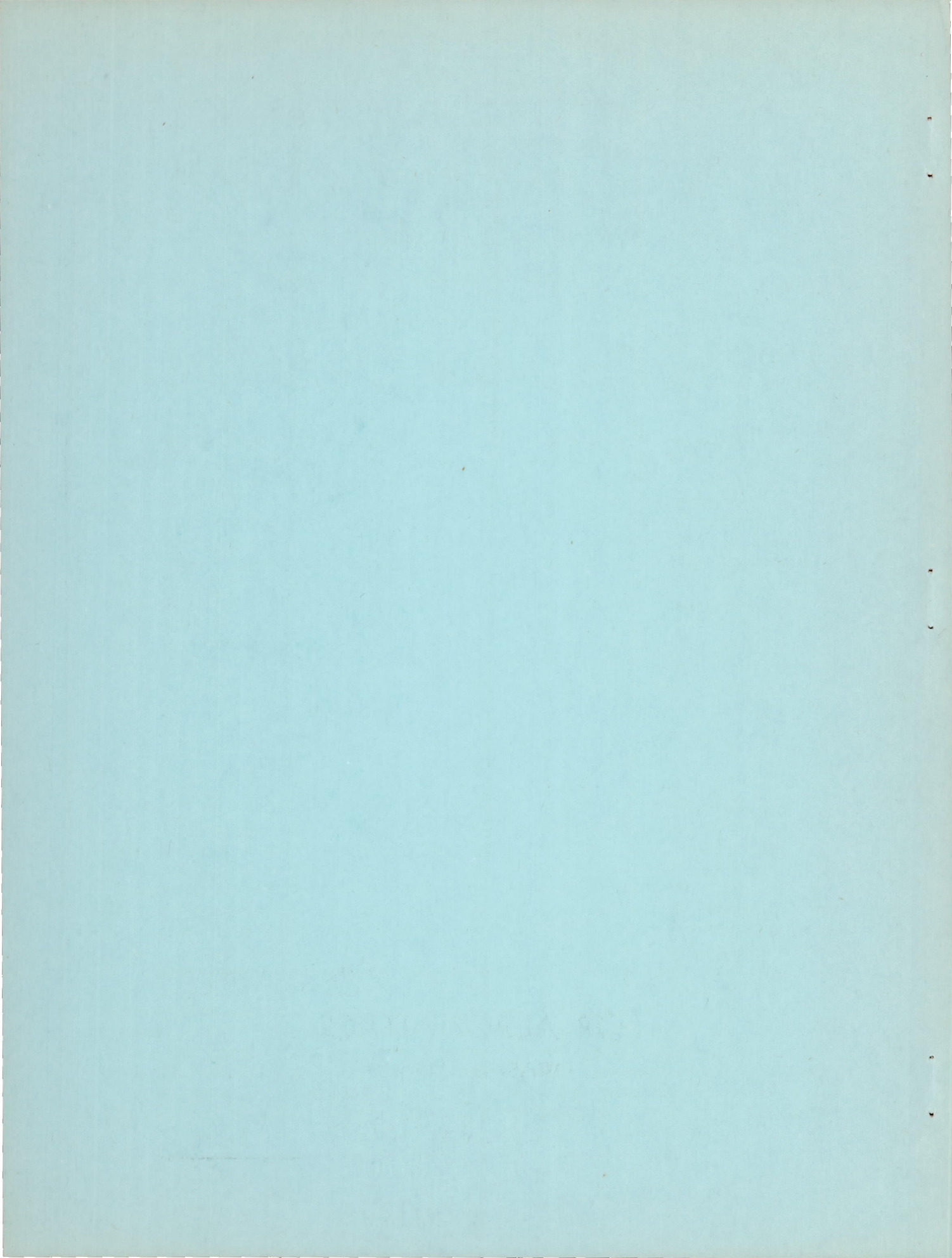NACA

RESEARCH MEMORANDUM

EFFECTS OF SLOT LOCATION AND GEOMETRY ON THE FLOW

IN A SQUARE TUNNEL AT TRANSONIC MACH NUMBERS

By William J. Nelson and James M. Cubbage, Jr.

Langley Aeronautical Laboratory
Langley Field, Va.

NATIONAL ADVISORY COMMITTEE
FOR AERONAUTICS
WASHINGTON

NATIONAL ADVISORY COMMITTEE FOR AERONAUTICS

RESEARCH MEMORANDUM

EFFECTS OF SLOT LOCATION AND GEOMETRY ON THE FLOW

IN A SQUARE TUNNEL AT TRANSONIC MACH NUMBERS

By William J. Nelson and James M. Cubbage, Jr.

SUMMARY

Data from an investigation of the effects of slot location and slot geometry on the flow in a square tunnel are presented for a Mach number range up to 1.4. These data are presented as curves of the center-line static-to-stagnation pressure ratio plotted as a function of the distance from the plane of the slot origin with the slots located in one, two, or four walls, or in the corners of a square tunnel. Calculated static-pressure and angle-of-flow distributions along the slotted boundary are presented for several slot configurations investigated in a tunnel with two opposite walls slotted. Knowledge of the static-pressure difference across the slots is shown to be inadequate to define the flow rate across the boundary. The data show that by maintaining a given distribution of open area, slots developed in one configuration may be applied to another with but minor changes in pressure distribution.

INTRODUCTION

The development of transonic test facilities has resulted in the design of slotted-wall tunnels differing widely in size and cross-sectional shape. Some of these are described in references 1 to 7. In the rectangular tunnels it has become customary to place the slots in the flat surfaces, whereas the corner locations have proved more usual with polygonal test sections. For each design, it has been necessary to develop by experiment a satisfactory slot shape and the final shapes differ widely from one tunnel to another as the test requirements, tunnel size, slot location, Mach number range, and Reynolds number vary.

The present investigation was initiated in the Internal Aerodynamic Branch of the Langley Laboratory to determine the effects of slot location on the pressure gradient in a square tunnel and to extend the slot-geometry studies reported in reference 7. In carrying out these objectives, a series of tests was conducted in which walls containing four identical slots were installed in one, two, or four sides of the tunnel,

and others in which the size of the individual slots was decreased as
the number of slotted walls increased, thus maintaining a given free-
area distribution in the direction of flow.   Similarly, when the slots
were moved to the corners, their width was increased to compensate for
the reduction in number of slots.   In a final test series, the geometry
of the individual slots was varied systematically, first increasing the
width at the upstream end of the tapered section, and then by shortening
the distance over which the width and depth were variable.   In investi-
gating the effects of changing peripheral location of the slots, it was
found impractical to develop an optimum slot for each configuration; how-
ever, a sufficient number of tests were conducted to establish a rela-
tionship between the different configurations by means of which slots
giving satisfactory results in one installation may be used to obtain
generally similar results in another.

Inasmuch as the pressure distribution along the tunnel axis is
determined by the rate of flow through the slots, the flow direction and
the pressure distribution along the slotted wall have been calculated
for the configurations for which the flow may be considered two dimen-
sional.   The complex nature of the flow generated with slots in four
walls or in the four corners precludes similar calculations for those
configurations.   However, from a correlation of the rate of flow through
the wall and the local pressure increment across the wall, it is possi-
ble to obtain a general picture of dependence of slot characteristics
upon slot geometry.

SYMBOLS

d_s depth of slot in untapered part of slot, in.

h effective height of tunnel, in.

L length of tapered part of slot, in.

M Mach number corresponding to p/P_o

M_c Mach number corresponding to p_c/P_o

n number of slots in each slotted wall

n_t total number of slots in tunnel periphery

P_o stagnation pressure

p local static pressure

p_c chamber static pressure

p_w average static pressure along slotted wall at any station

W ratio of open to closed area for untapered slotted part of
             an individual slotted wall, nw_s/w

w effective width of tunnel, in.

w_s maximum width of slot, in.

w_{s_x} width of slot at any point x, in.

x distance along tunnel measured from upstream end of slot, in.

θ_w angle of flow relative to slotted wall; positive out through
             the wall, deg

Φ slot taper included angle, deg

APPARATUS

Photographs of the tunnel used in this investigation are presented
as figure 1. The top part of the plenum chamber and tunnel side plate
have been removed in figure 1(a) in order to show the general assembly
of the model with the static-pressure probe installed. The inlet bell
shown provided a smooth and gradual fairing into the tunnel sides and
nozzle blocks. The test channel had a $4\frac{1}{2}$ - inch-square cross section
which remained constant from the downstream end of the nozzle blocks to
the beginning of the exit diffuser, a distance of 17 inches. The diam-
eter of the cylindrical plenum chamber surrounding the tunnel was
30 inches. Figure 1(b) shows a close-up view of the tunnel with slots
located in the corners. The wooden blocks that carried the exit-diffuser
contour forward to the end of the slots for slotted-corner tunnel con-
figurations were shaped to allow some of the air in the slots to flow
into the diffuser. All other configurations reported herein had small
filler blocks with sharp leading edges between the bars at the end of
the slots to turn all the air in the slots toward the chamber. One type
of these filler blocks can be seen in figure 1(c) in which the 1/8-open,
0.141-inch-width, 2.75° tapered entry variable-depth-slot configuration
is shown. It is noted from this figure that the downstream end of the
slotted walls is cut down slightly to extend the diffuser forward almost
to the end of the slots.

The variation of the free-area ratio for an individual slotted wall
along the tapered part of the slot with distance from the upstream end

of the slot is shown in figure 2. The series of parallel solid lines in figure 2 represents slots of rectangular plan form in which the length of the tapered part was varied in order to provide slots the width of which, at the origin, varied from 0 to 0.141 inch; thus, slots with free-area ratios of 0, 1/25, 1/12, and 1/8 at their origins opened along a 2.75° angle to one-fifth of the wall area. The curve for the 0.113-inch-width, 1.38° tapered slots in the side walls coincides with that for the 0.432-inch-width, 5.24° tapered slots in the corners (see fig. 2). The 1.46° taper for the 0.432-inch-width corner slot extends the full 17-inch length of the tunnel. Significant dimensions and ratios for the tunnel and slot configurations investigated are presented in table I along with the numbers of the corresponding data figures.

The static-pressure probe and actuating mechanism were attached to the exit diffuser in order to permit the inlet bell, tunnel, exit diffuser, and survey probe to be removed from the plenum chamber as a unit. The static-pressure probe had four 0.0135-inch-diameter orifices equally spaced around the circumference of a station located 10 tube diameters behind the base of the $6\frac{1}{2}°$ conical tip. The outside diameter of the tube was 0.060 inch. The probe had a maximum length of travel of $11\frac{1}{2}$ inches from its zero position which was set in the plane of the slot origin for most of the configurations reported herein. The reflection plane, used to double the effective height of the tunnel for two slot configurations, had 0.030-inch-diameter orifices spaced at $\frac{1}{2}$ - inch intervals along its center line and the static pressures from these orifices were recorded photographically from a multiple-tube manometer. Stagnation and plenum-chamber pressures were read from mercury-filled U-tubes and the static pressure in the plenum chamber was set and maintained by adjustment of a remotely controlled vacuum system the operation of which was completely independent of the main stream power. Mach numbers of 1.0 to 1.4, the limit of these tests, were obtained at a constant stagnation pressure of 2 atmospheres; the corresponding stagnation temperature was approximately 250° F.

RESULTS

The results of this investigation, presented in figures 3 to 6 as static-pressure distributions along the tunnel center line for a range of chamber to stagnation pressure ratios p_c/P_0, extend the slot-geometry studies of reference 7 (figs. 3 and 4) and show the effects of slot location (figs. 4 to 6). The abscissa of these figures is the distance along the tunnel from the origin of the slot expressed in terms of the effective tunnel height. The pressure distributions presented in figure 3

were obtained with a slotted wall in only one side of the square tunnel the effective height of which was twice its width. The slotted wall used in obtaining the data of figure 3(a) carried four slots the width of which increased from 0 to 0.225 inch along a 2.75° angle and continued at constant width through the remainder of the tunnel. The subsonic pressure was nearly constant from the slot origin to a point approximately one tunnel height downstream but increased rapidly from this point back. Unpublished results from other experiments indicate that this rise in pressure in the downstream part of the slotted section at subsonic velocities accompany operation at low chamber pressure with low pressure ratio across the tunnel. At all supersonic speeds within the range of this investigation, the air expanded smoothly to pressures equal to or below the chamber pressure with the resulting overexpansion followed by nonuniform flow. In the supersonic range, changes in slot geometry were necessary to effect significant improvements in pressure distribution. Figure 3(b) shows results obtained when the maximum slot width was decreased to 0.141 inch (one-eighth-open wall) and the depth decreased linearly from 1/2 to 1/16 inch over the region of increasing slot width. In effecting this modification, the slot origin was moved rearward increasing the constant-area approach section from 1 inch to 2.75 inches; the displacement of the curves in this region is attributed to boundary-layer effects resulting from this modification. Reducing the free area of the boundary, together with the change in slot depth, resulted in substantial improvement in the pressure distribution, virtually eliminating both the subsonic pressure rise near the back of the tunnel and the initial overexpansion at supersonic Mach numbers. At the higher Mach numbers failure to reach the chamber pressure within the limits of these surveys suggests that choking in the slots was imminent.

The results obtained when the slot configurations of figure 3 and several others were mounted in two opposite walls of this square tunnel are presented in figure 4. Figures 4(a) to 4(d) present a series of distributions obtained by modification of slots the width of which increased uniformly from 0 to 0.225 inch in a distance approximately equal to the tunnel height, $L/h = 1.05$. The effects of ratios of abrupt slot opening to free area of one-twenty-fifth, one-twelfth, and one-eighth of the wall area are shown in figures 4(b), 4(c), and 4(d), respectively. The rate of initial expansion increased with the initial slot area but little difference in the distributions is to be noted downstream of the initial expansion. Distributions for a configuration with slots the width and taper angle of which were half as large as those of figure 4(a) show a decrease in the initial rate of expansion and also in the amount of overexpansion and subsequent recompressions; the general shapes of the distributions, however, are similar. Compare figures 4(a) and 4(e). The slot configurations of figures 4(f) and 4(g) were of identical plan form but differed in the slot depth which was constant (1/2 inch) in figure 4(f) but for figure 4(g) decreased linearly from 1/2 inch to 1/16 inch along the region of increasing width and continued at the

$\frac{1}{16}$ - inch depth from this point to the end of the slot. These two fig-
ures were originally presented in reference 7; they are repeated here
for completeness and to facilitate comparisons. The abruptness and
magnitude of the recompressions shown in figure 4(f) have been reduced
significantly and the flow has been improved generally by the intro-
duction of variable depth in the slots. Reduction of the taper length
of the slots presented in figure 4(g) by 50 percent resulted in the
distribution shown in figure 4(h) which shows a slightly greater rate
of expansion with some improvement in the flow at all Mach numbers
investigated.

The installation of slotted walls in all four sides of the tunnel
resulted in the center-line pressure distributions presented in figure 5.
With one-fifth open walls, similar to those used in one and two sides of
the tunnel (see figs. 3(a) and 4(a)) the pressure at subsonic Mach num-
bers was uniform; at supersonic speeds, however, the initial over-
expansion was substantially greater than that encountered in previous
tests and the subsequent pressure differences along the tunnel were
large. With one-tenth open walls, as used in the tests represented in
figure 4(e), the subsonic flow was again uniform and the supersonic
pressure distribution, although unsatisfactory (fig. 5(b)), was markedly
improved over that obtained with the more open walls of figure 5(a).

In the various polygonal tunnels from which data are available, the
slots have, in general, been located in the corners rather than in the
flat surfaces. Results of tests of a square tunnel with corner slots
are presented in figure 6. Slot depth was constant for figures 6(a) and
6(b), the width, however, varied from 0 to 0.432 (W = 1/10) along taper
angles of 1.46° and 5.24°, respectively. The slots shown in figures 6(c)
and 6(d) were of constant width throughout, with the sides diverged at
an angle of 90° as shown in table I, sketch 5.

DISCUSSION

Effect of tunnel height-width ratio.- Typical center-line pressure
distributions in tunnels of different height-width ratios with one-fifth-
and one-eighth-open slotted walls are presented in figures 7(a) and 7(b),
respectively. A height-width ratio of 1.0 was obtained by setting iden-
tical slotted walls in opposite sides of the tunnel; a single slotted
wall with a reflection plane was used to double the effective height of
the tunnel, h/w = 2.0. In both figures solid lines represent data from
figure 4, h/w = 1.0, and dotted lines represent data from figures 3,
h/w = 2.0. At each Mach number, the pressure drop accomplished in the
initial expansion was smaller for the tunnel of greater height-width
ratio. This difference is a result of greater flow constriction resulting

from increased boundary-layer displacement which, as discussed in reference 7, accompanies the decrease in slot area relative to the wetted area of the tunnel. Because of the reduced expansion in the tunnel of greater height, the flow through the test section was generally more uniform at $\frac{h}{w} = 2.0$ than at $\frac{h}{w} = 1.0$.

The slope of the nondimensional pressure gradient was also observed to increase as the height-width ratio of the tunnel increased. Data presented in reference 7 showed that the rate at which the initial expansion is effected was determined by the rate at which air is removed from the tapered section of the slots, thus an increase in pressure gradient accompanied a decrease in the ratio of slot taper length to tunnel height, L/h. To examine this effect quantitatively, one-eighth-open walls with a slot taper length of 1.5 inches were tested in opposite sides of the tunnel, figure 4(h). These data, superimposed on the curves of figure 7(b), are in excellent agreement with the dotted curves obtained when slots of the same free area in which the taper was twice as long were tested with the reflection plane doubling the effective height of the tunnel. In regions where the rate of flow through the slots is high, the effective height-width ratio of the tunnel is then of little significance; however, as the slot flow decreases downstream of the initial expansion, the increase in boundary displacement accompanying increases in h/w exerts an appreciable influence on the pressure distribution.

Effect of peripheral location of slots.- For many applications, it appears desirable to slot all walls of the test section in order that the interference effects might be more uniformly distributed when testing three-dimensional models. Typical pressure distributions obtained with one-fifth-open slotted walls installed in all four sides of the tunnel are shown in figure 7(c) superimposed on curves obtained when similar walls were set opposite each other. The differences between corresponding curves reflect not only the influence of slotted-wall location but also the effect of the accompanying increase in slot area. A similar comparison between results obtained when the width of individual slots used with four slotted walls was reduced by 50 percent, thus maintaining the free-area distribution of the tunnel with one-fifth-open walls set opposite each other, (presented in fig. 7(d)) shows relatively little difference in the flow along the axis. The small differences which exist must be attributed in part to the change in slot width necessary to maintain equal free area in both tunnels. The parallelism of the latter curves suggests that both this effect and the effect of slotted-wall location are small.

In order to facilitate the correlation of data from tests in rectangular tunnels in which slots are usually located in the flat surfaces with data from tests in polygonal tunnels where slots are usually installed in the corners, a comparison is presented in figure 7(d). These curves

also are consistent with those obtained with slots in the flat surfaces only. The small differences between curves may be attributed to the combined influence of the increase in slot width and the decrease in angle between the edge of the slot and the adjacent wall of the tunnel, as well as to the change in slot location. The observed similarity of curves obtained with slots of a given free-area distribution located in two or four sides of a square tunnel, or in the corners, leads to the general conclusion that, at Mach numbers below 1.35, the flow in slotted tunnels is to a first order determined by the longitudinal distribution of the slot area, and that the peripheral location of the slots is of relatively little importance in determining the pressure distribution along the tunnel axis.

Effect of slotted-area distribution.- The center-line pressure distributions obtained with slotted walls set opposite each other have been used as a starting point to determine the effect of slotted-area distribution on the rate of flow through a slotted boundary. This tunnel configuration was selected in order that the problem might be simplified to one of two-dimensional flow and as a further simplification the effects of viscosity have been neglected. The results are presented in figures 8(a) to 8(g) with the measured center-line pressure at $M \approx 1.1$, 1.2, and 1.35 given at the top of each figure followed by characteristics nets at two Mach numbers and by the calculated flow direction and pressure distribution along the slotted wall. Along the one-fifth-open wall with slots tapered from 0 to 0.225 inch (fig. 8(a)), the flow angle increased to a maximum value on the order of 1/2 to 3/4 of the deviation corresponding to a Prandtl-Meyer expansion to the chamber pressure with excessive air removal effected at all Mach numbers resulting in a reversal in direction of flow through the floor farther downstream. This invariably resulted in large pressure (Mach number) variations along the tunnel. The region of overexpanded flow increased with Mach number resulting at $M_c = 1.36$ in the attainment of more or less uniform flow at $M > 1.4$ for an axial distance equal to approximately one-half the tunnel height. In these regions of overexpansion, the calculations frequently indicate flow into the slots in the presence of an adverse static-pressure difference; this flow into the slots can obviously occur only if the dynamic pressure of the entering air is being converted to static pressure through diffusion within the slots. Such diffusion is readily effected in tapered slots of appreciable depth.

A similar analysis of data obtained in three configurations with slots opening abruptly to provide in four slots an area equal to one-twenty-fifth, one-twelfth, and one-eighth of the wall area and increasing along a straight 2.75° taper to one-fifth of the wall area is presented in figures 8(b) to 8(d). These curves show that a higher initial rate of expansion is associated with the abrupt opening slots and that the amount of expansion effected at this higher rate increases with initial slot width; the pressure distribution along the tunnel, however, was not

significantly changed by these slot modifications. These figures indicate that the expansion to supersonic Mach numbers was initiated at a point approximately $\frac{1}{2}$ inch (x/h = 0.1) downstream from the abrupt slot opening. This downstream displacement of the initial expansion is attributed to possible flow reversal within the slots resulting from the static-pressure rise in the diverging slots; flow reversal can probably occur only in slots of appreciable depth-width ratio since the stream tube divergence within the slots would decrease with decreasing slot depth.

Comparison of the curves of θ_w plotted against x/h in figures 8(a) and 8(e) shows that a 50-percent reduction in slot width throughout the entire length resulted in substantial reductions in flow angularity relative to the wall and an increase in the area over which the air was removed from the tunnel. Spreading this region of outflow over a greater distance and decreasing the flow angularity along the wall resulted in smaller pressure differences throughout the tunnel. In figure 8(f), data from tests with one-eighth-open walls are analyzed. In this configuration, as in that shown in figure 8(a), the slot width increased along a 2.75° taper from 0 to 0.141 inch; the free area of the one-fifth- and one-eighth-open walls increased at the same rate. In this part of the wall, the rate of air removed from the tunnel was essentially independent of the ultimate slot width; farther downstream, however, the pressure distribution was somewhat improved as the amount of overexpansion was reduced by reducing maximum slot width.

In an effort to reduce the overexpansion without decreasing the slot area or increasing the taper length, tests were made in which slot depth was reduced linearly through the tapered region to reduce the subsonic diffusion effected in the diverging section of each slot and to reduce the local flow coefficient of the slots. Figure 8(g) shows that the initial overexpansion, although still present, is significantly less than in the comparable configuration with slots of constant depth, figure 8(f). The pressure distribution along the tunnel was substantially improved by reducing slot depth through the region of variable width.

Flow through slots.- Many attempts have been made to determine the pressure distribution in slotted tunnels analytically from a knowledge of the flow characteristics of the slots themselves. In reference 8, the static-pressure difference and the flow characteristics of a porous-walled tunnel were used to calculate tunnel empty pressure distributions; the results were consistent with experimental data. In reference 5, it is shown that, with the assumption of an orifice coefficient on the order of 0.85, it was also possible to calculate the trend of the pressure distribution in slotted tunnels, provided the slot depth was very small in proportion to its width. Similar calculations using the slot configurations reported here were impossible, since, as previously discussed,

regions were encountered in which the direction of flow was counter to
the static-pressure difference. The mean flow angularity to the slotted
wall at the end of the tapered section of the slots, as a function of the
static-pressure difference across the wall, is presented for several con-
figurations in figure 9. The four curves of figure 9(a) show different
characteristics at the same tunnel cross section; the displacement of the
curves results solely from slot changes ahead of the measuring station.
Note that, in the first and third quadrants, the direction of flow is
consistent with the static-pressure difference. The region of counter-
flow in the second quadrant decreases as the length of the tapered sec-
tion of the slots decreases (shown at the top of the figure); with slots
opening abruptly to 0.141 inch (one-eighth open) no reverse flow occurred
at the reference station. Decreasing taper length by filling the forward
part of the slots decreases the diffusion which may occur in the slots
proper since the entrance area increases, whereas the exit area remains
constant. Because of the decrease in slot length ahead of the reference
station, a very high rate of turning would be necessary for air entering
the front of the slot to fill the tapered section of the slot; for this
reason, it appears probable that the rate of flow through the slot at
this cross section decreases as the taper length is reduced. The exist-
ence of such a wide range of flow rates for a given static-pressure dif-
ference at a fixed-slot cross section precludes calculation of pressure
distributions in slotted-wall tunnel with slots of appreciable depth.
Although knowledge of the dynamic pressure of the air in the slots is
essential to evaluation of the rate of flow into the slot, it is not
obvious that even this information is sufficient for calculation of tun-
nel pressure distributions.

Similar curves drawn at the end of the tapered section for slots
opening from 0 to 0.141 inch (one-eighth open) along a 2.75° taper are
drawn in figure 9(b). The curve at the left is drawn for slots of con-
stant depth, that on the right for slots the depth of which decreased
linearly from 1/2 to 1/16 inch as the width increased. With these slot
configurations, the regions of flow counter to the static-pressure dif-
ference were virtually eliminated. The rate of flow into the $\frac{1}{16}$-inch-
deep slot was consistently less than that through the $\frac{1}{2}$-inch slot of
the same width and at the same static-pressure difference. The decreased
slope of the curve obtained with variable depth in the tapered part of
the slot at the higher flow rates indicates a maximum flow rate corre-
sponding to less than 3° deviation probably because of choking in the
tapered part of the slots. It is not surprising that the flow charac-
teristics of the slotted wall vary with depth of the slots. Much more
experimentation will be required, however, before this effect can be
evaluated quantitatively.

This discussion is necessarily general; however, it does serve to
point out some of the parameters which introduce great difficulty into

the analysis of slotted walls. The unpredictable nature of the slot flow complicates the calculation of wall-interference effects and of shock-reflection characteristics of slotted walls. It is apparent that increasing slot depth increases the dependence of the performance on the dynamic pressure of the slot air. Maximum conversion of this dynamic pressure to static pressure, however, seems necessary to the reduction of high-power requirements of slotted wind tunnels; this conversion is most desirable in the upstream section of the tunnel where high transverse flow rates are necessary to the generation of supersonic Mach numbers.

CONCLUSIONS

From the results of this experimental investigation of the effects of slot location and geometry on the flow in a square tunnel at transonic Mach numbers, it is concluded that:

1. The pressure distribution along the tunnel axis at transonic speeds is determined primarily by the axial distribution of the slot area and is essentially independent of the peripheral location of the individual slots.

2. In rectangular tunnels, slotted top and bottom, the maximum Mach number attainable with slotted walls of a given free-area ratio decreases as the height-width ratio of the tunnel increases because of increased boundary-layer constriction effects.

3. Knowledge of the local static-pressure difference across a slotted boundary does not permit calculation of the transverse flow rate through that boundary.

Langley Aeronautical Laboratory,
National Advisory Committee for Aeronautics,
Langley Field, Va., September 30, 1953.

REFERENCES

1. Wright, Ray H., and Ward, Vernon G.: NACA Transonic Wind-Tunnel Test
     Sections. NACA RM L8J06, 1948.

2. Wright, Ray H., and Ritchie, Virgil S.: Characteristics of a Tran-
     sonic Test Section With Various Slot Shapes in the Langley 8-Foot
     High-Speed Tunnel. NACA RM L51H10, 1951.

3. Ward, Vernon G., Whitcomb, Charles F., and Pearson, Merwin D.: Air-
     Flow and Power Characteristics of the Langley 16-Foot Transonic
     Tunnel With Slotted Test Section. NACA RM L52E01, 1952.

4. Goethert, Bernhard H.: Investigations on Transonic Test Sections at
     the Wind Tunnel Branch, AMC-Wright Field. Air Materiel Command,
     Wright Field, Sept. 25, 1950.

5. Osborne, James I., and Zeck, Howard: Progress Report on Development
     of a Transonic Test Section for the Boeing Wind Tunnel (BWT 188).
     Vol. I - December 1950 to June 1951. Doc. No. D-11955, Boeing
     Airplane Company, Sept. 1951.

6. Nelson, William J., and Bloetscher, Frederick: Preliminary Investi-
     gation of a Variable Mach Number Two-Dimensional Supersonic Tunnel
     of Fixed Geometry. NACA RM L9D29a, 1949.

7. Nelson, William J., and Cubbage, James M., Jr.: Effects of Slot Size
     and Geometry on the Flow in Rectangular Tunnels at Mach Numbers up
     to 1.4. NACA RM L53B16, 1953.

8. Nelson, William J., and Klevatt, Paul L.: Preliminary Investigation
     of Constant-Geometry, Variable Mach Number, Supersonic Tunnel With
     Porous Walls. NACA RM L50B01, 1950.

TABLE I.— DIMENSIONS AND LOCATION OF SLOT CONFIGURATIONS INVESTIGATED.

h, in.	$\frac{h}{w}$	$\frac{nw_s}{w}$	$\frac{n_t w_s}{2(h+w)}$	w_s, in.	d_s, in.	n	Φ, deg	Taper $w_{s_{x=0}}$ to $w_{s_{x=L}}$	$\frac{L}{h}$	Slot separation, in.	Slot total length, in.	Slot location	Figure number
9.0	2.0	1/5	1/20	0.225	0.500	4	2.75	0 to 0.225	0.52	0.90	16.0	1	3(a)
9.0	2.0	1/8	1/32	.141	.063	4	2.75	0 to 0.141	.33	.90	12.8	1	3(b)
4.5	1.0	1/5	1/10	.225	.500	4	2.75	0 to 0.225	1.05	.90	16.0	2	4(a),8(a)
4.5	1.0	1/5	1/10	.225	.500	4	2.75	0.045 to 0.225	.84	.90	15.0	2	4(b),8(b)
4.5	1.0	1/5	1/10	.225	.500	4	2.75	0.094 to 0.225	.61	.90	14.0	2	4(c),8(c)
4.5	1.0	1/5	1/10	.225	.500	4	2.75	0.141 to 0.225	.39	.90	13.0	2	4(d),8(d)
4.5	1.0	1/10	1/20	.113	.500	4	1.38	0 to 0.113	1.05	1.01	16.0	2	4(e),8(e)
4.5	1.0	1/8	1/16	.141	.500	4	2.75	0 to 0.141	.66	.90	12.8	2	4(f),8(f)
4.5	1.0	1/8	1/16	.141	.063	4	2.75	0 to 0.141	.66	.90	12.8	2	4(g),8(g)
4.5	1.0	1/8	1/16	.141	.063	4	5.50	0 to 0.141	.33	.90	13.0	2	4(h)
4.5	1.0	1/5	1/5	.225	.500	4	2.75	0 to 0.225	1.05	.90	16.0	3	5(a)
4.5	1.0	1/10	1/10	.113	.500	4	1.38	0 to 0.113	1.05	1.01	16.0	3	5(b)
4.5	1.0	1/10	1/10	.432	.500	1	1.46	0 to 0.432	3.78	—	17.0	4	6(a)
4.5	1.0	1/8	1/8	.540	.354	1	5.24	0 to 0.432	1.05	—	17.0	4	6(b)
4.5	1.0	1/10	1/10	.432	.354	1	180	None	0	—	17.0	5	6(c)
4.5	1.0	1/10	1/10	.432	.354	1	180	None	0	—	17.0	5	6(d)

Section A-A

— — — — Reflection plane containing static-pressure orifices

⊙ Probe position

∖∖∖∖∖ Solid boundary

① ② ③ ④ ⑤
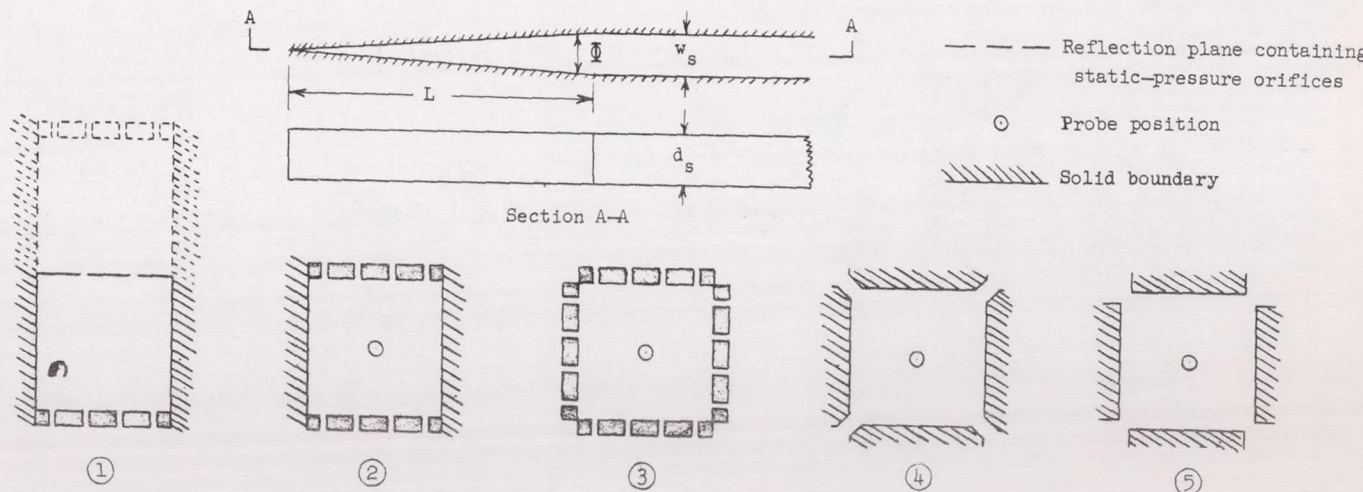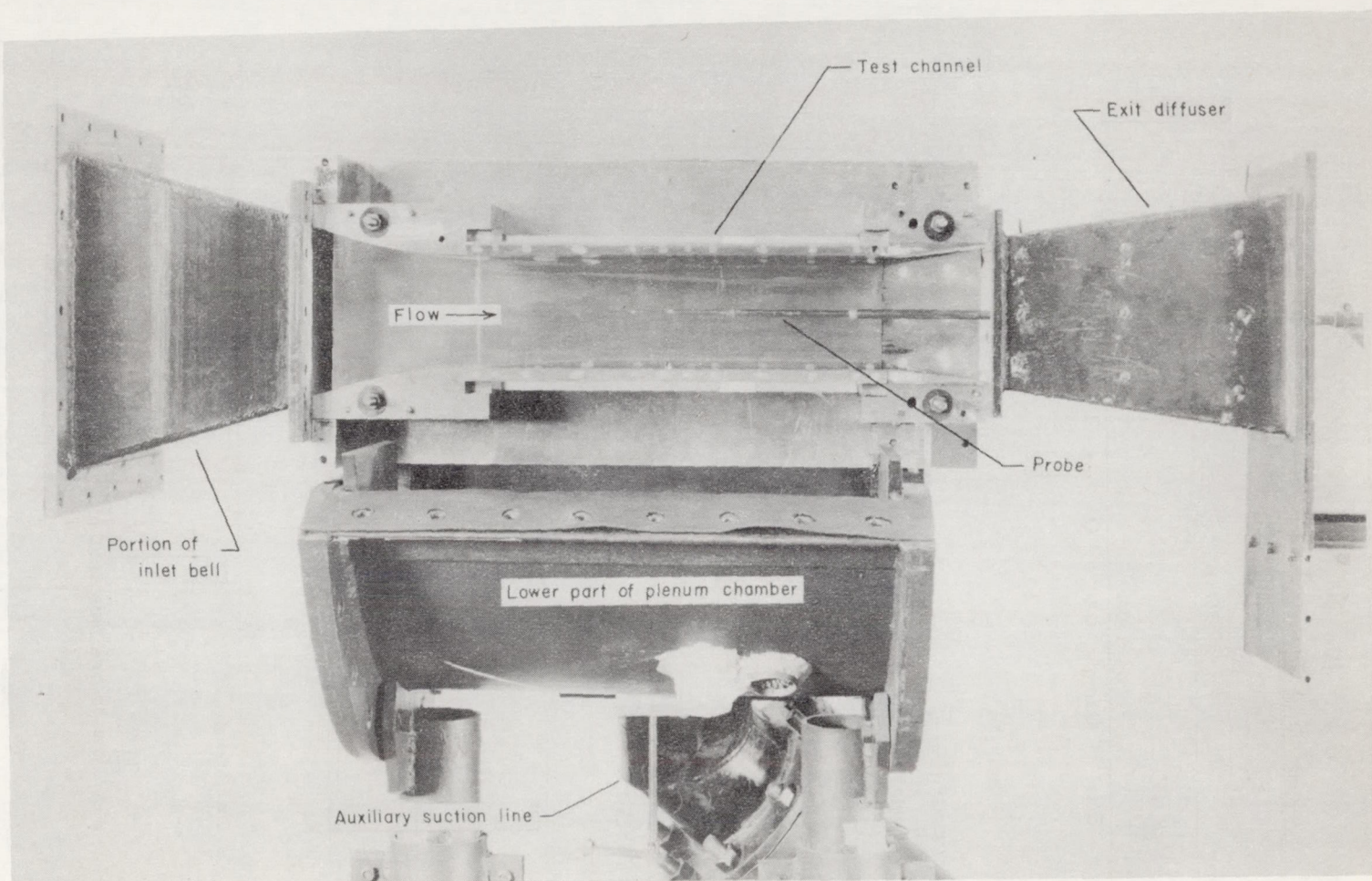
L-78902.1

(a) Partial assembly of test equipment.

Figure 1.- Test equipment.
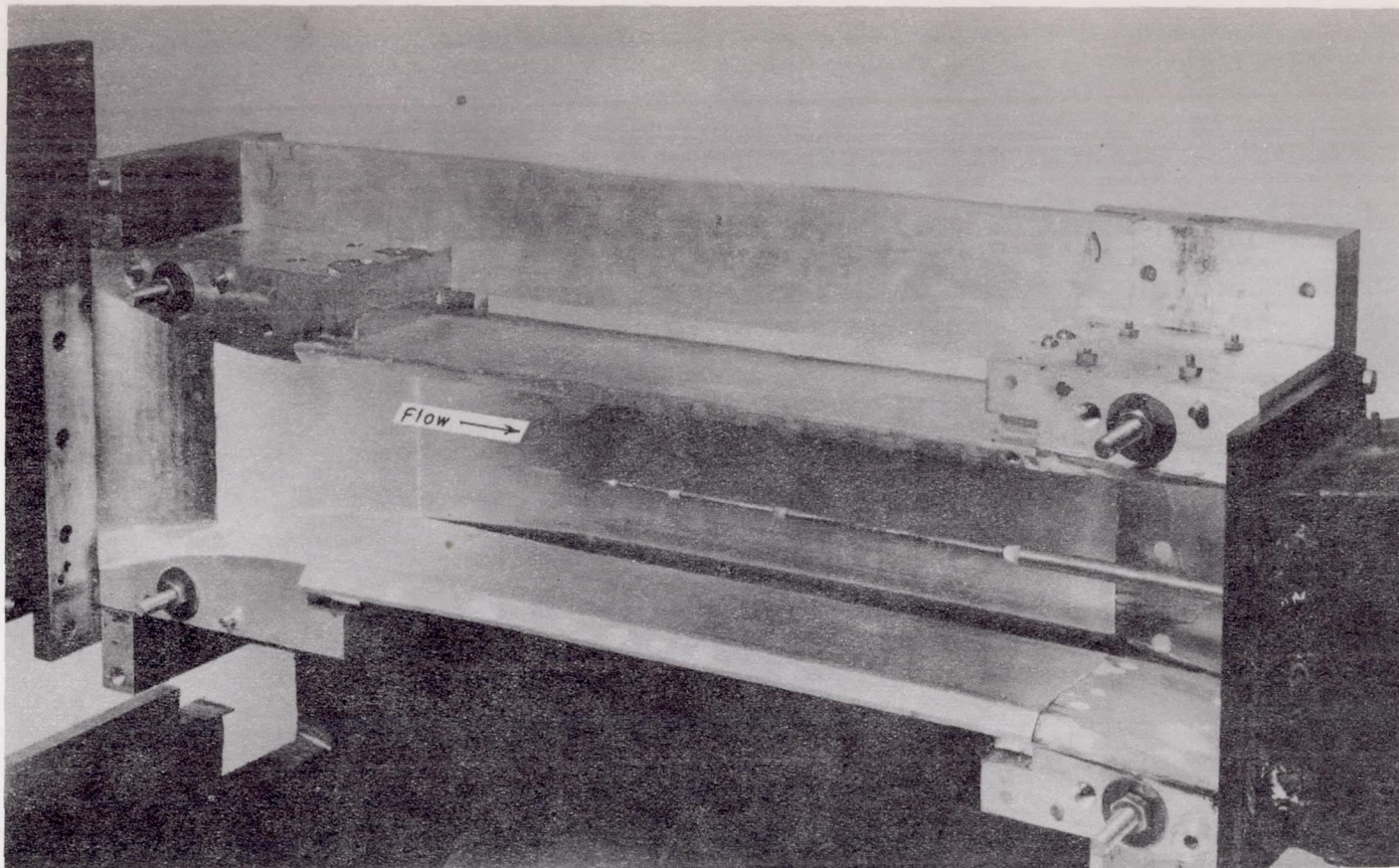
L-78903.1

(b) Detailed view of corner slot configuration; $\frac{nw_s}{w} = \frac{1}{10}$; $w_s = 0.432$ inch;
$\Phi = 5.24^\circ$.

Figure 1.- Continued.
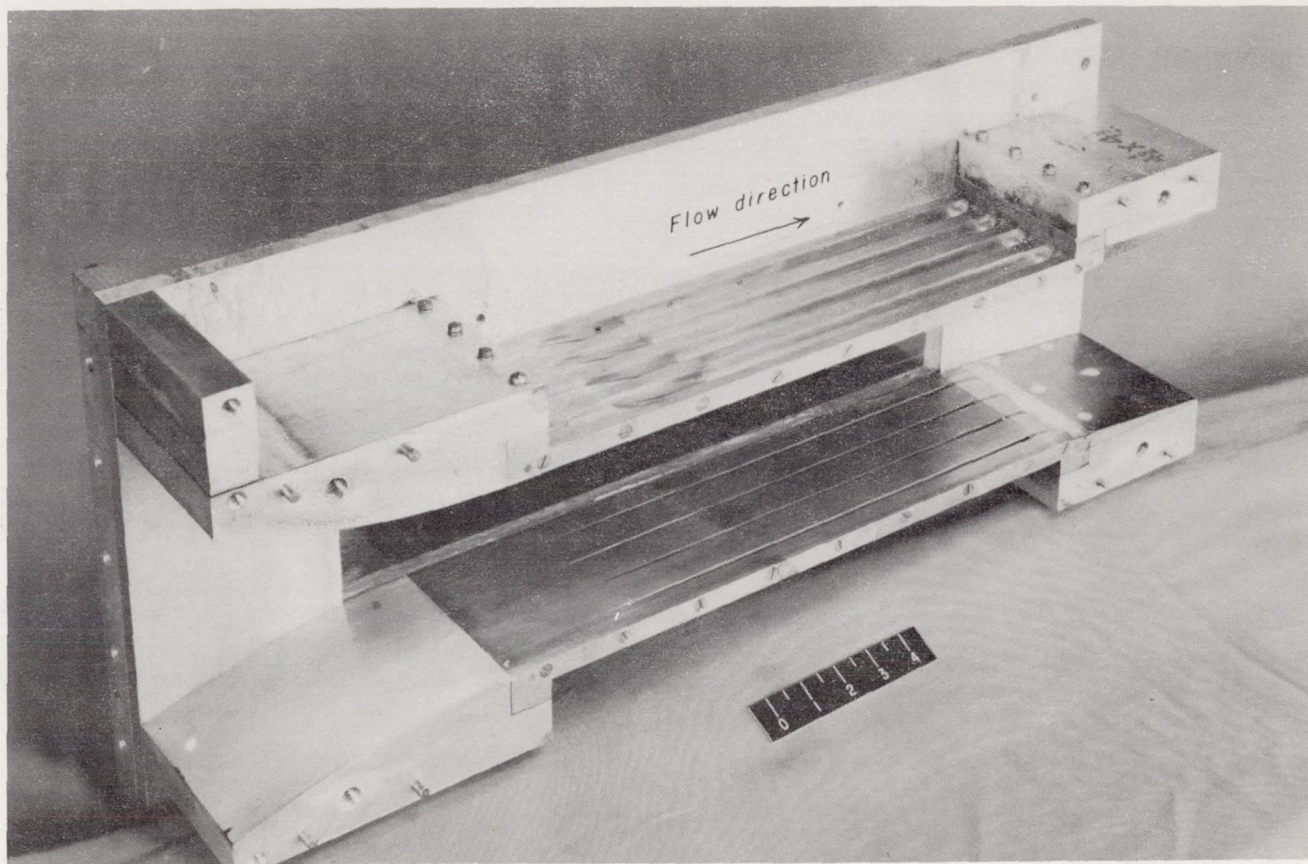
L-76593.1

(c) Detailed view of variable-slot-depth configuration; $\frac{nw_S}{w} = \frac{1}{8}$;

$w_S = 0.141$ inch; $\Phi = 2.75^{\circ}$.

Figure 1.- Concluded.
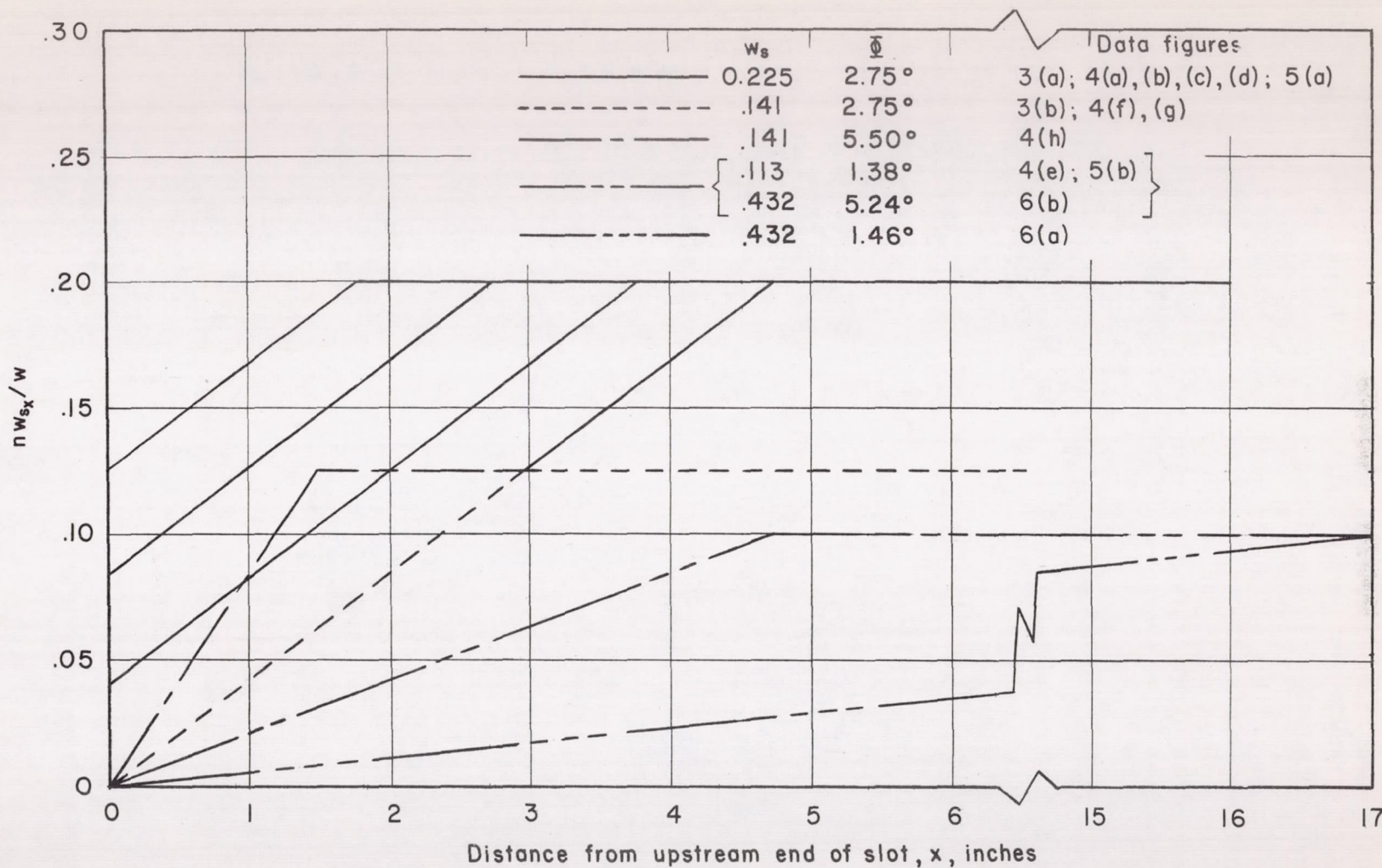
Figure 2.- Variation of free area ratio along tapered part of slot with
distance from upstream end of slot.
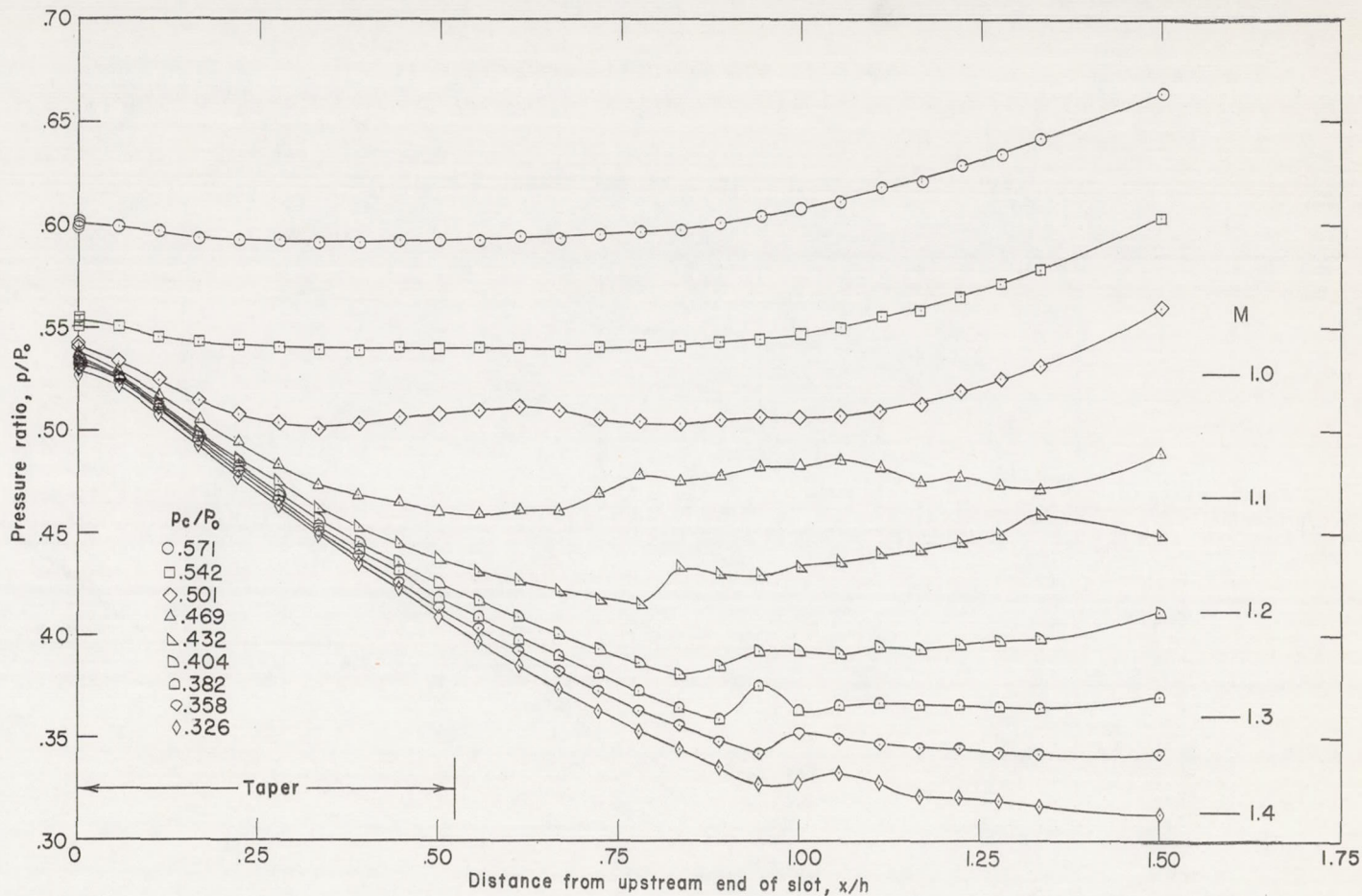
(a) $\dfrac{nw_S}{w} = \dfrac{1}{5}$; $w_S = 0.225$ inch; $\Phi = 2.75^{\circ}$.

Figure 3.- Pressure distribution along reflection plane; h = 9 inches;
$w = 4\dfrac{1}{2}$ inches.
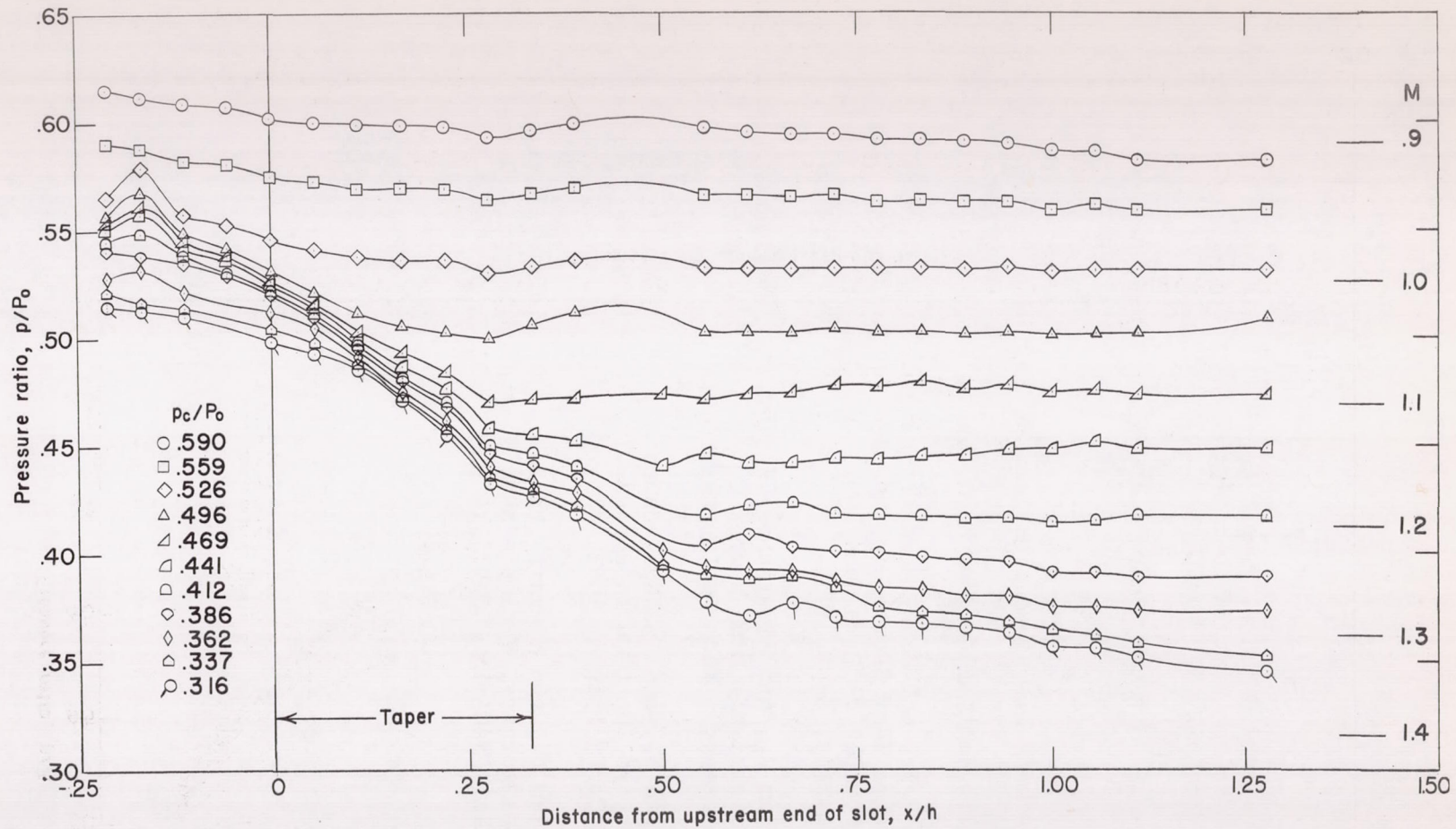
(b) $\dfrac{nw_s}{w} = \dfrac{1}{8}$; $w_s = 0.141$ inch; $\Phi = 2.75^\circ$; variable depth along taper.

Figure 3.- Concluded.
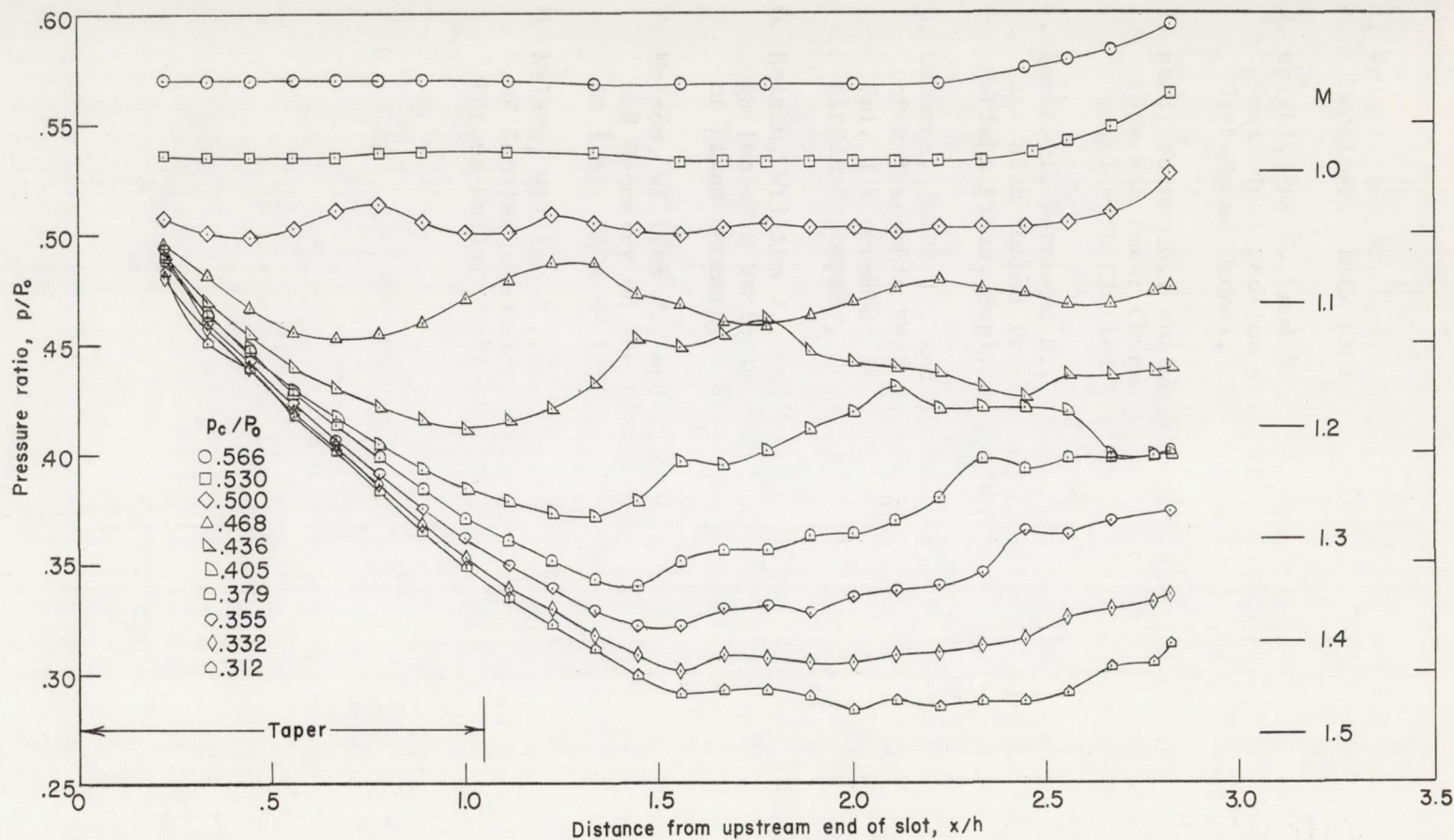
(a) $\dfrac{nw_s}{w} = \dfrac{1}{5}$; $w_s = 0.225$ inch; $\Phi = 2.75^\circ$; taper = 0 to 0.225 inch.

Figure 4.- Pressure distribution along center line (two walls slotted); $w = 4\frac{1}{2}$ inches; $h = 4\frac{1}{2}$ inches.
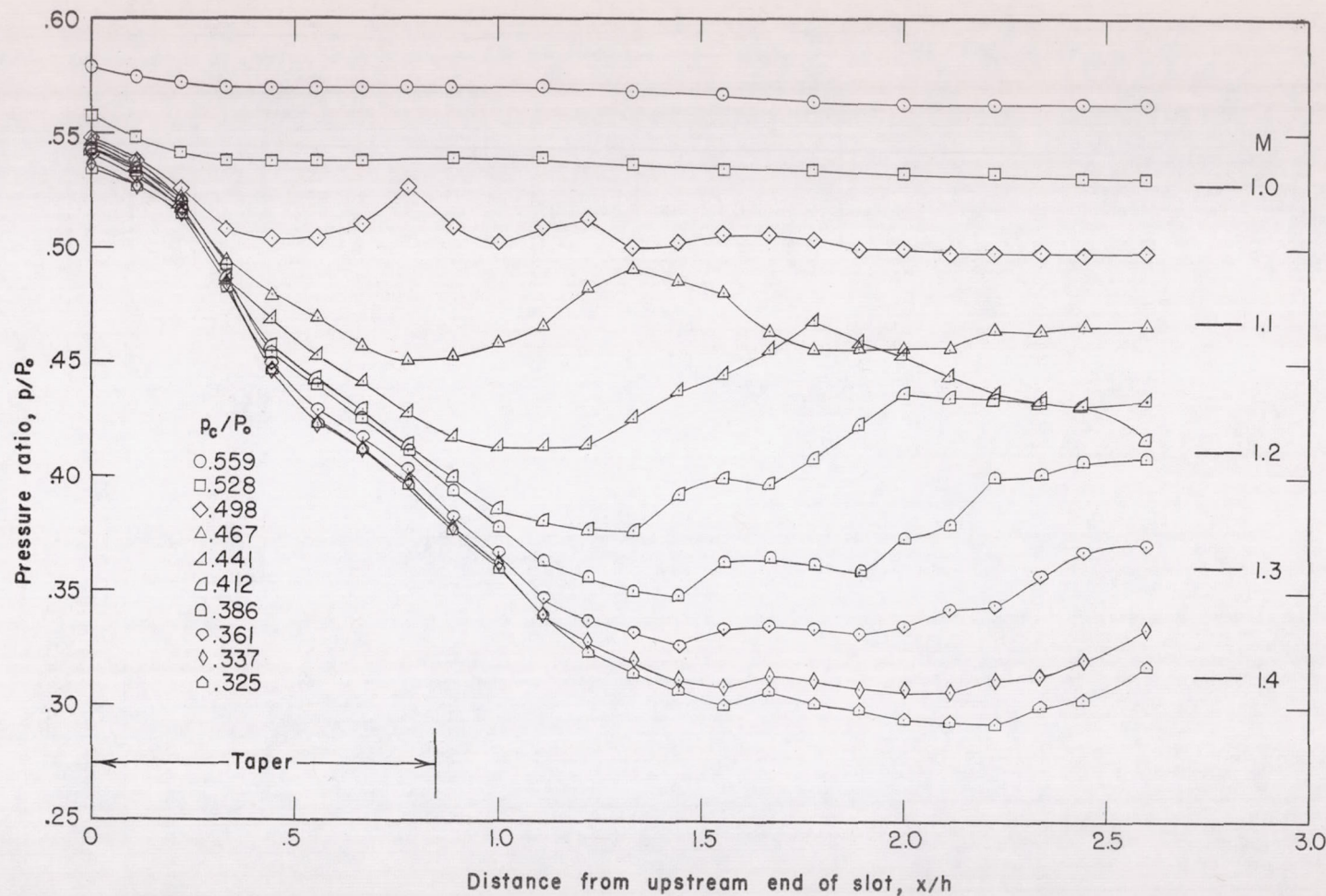
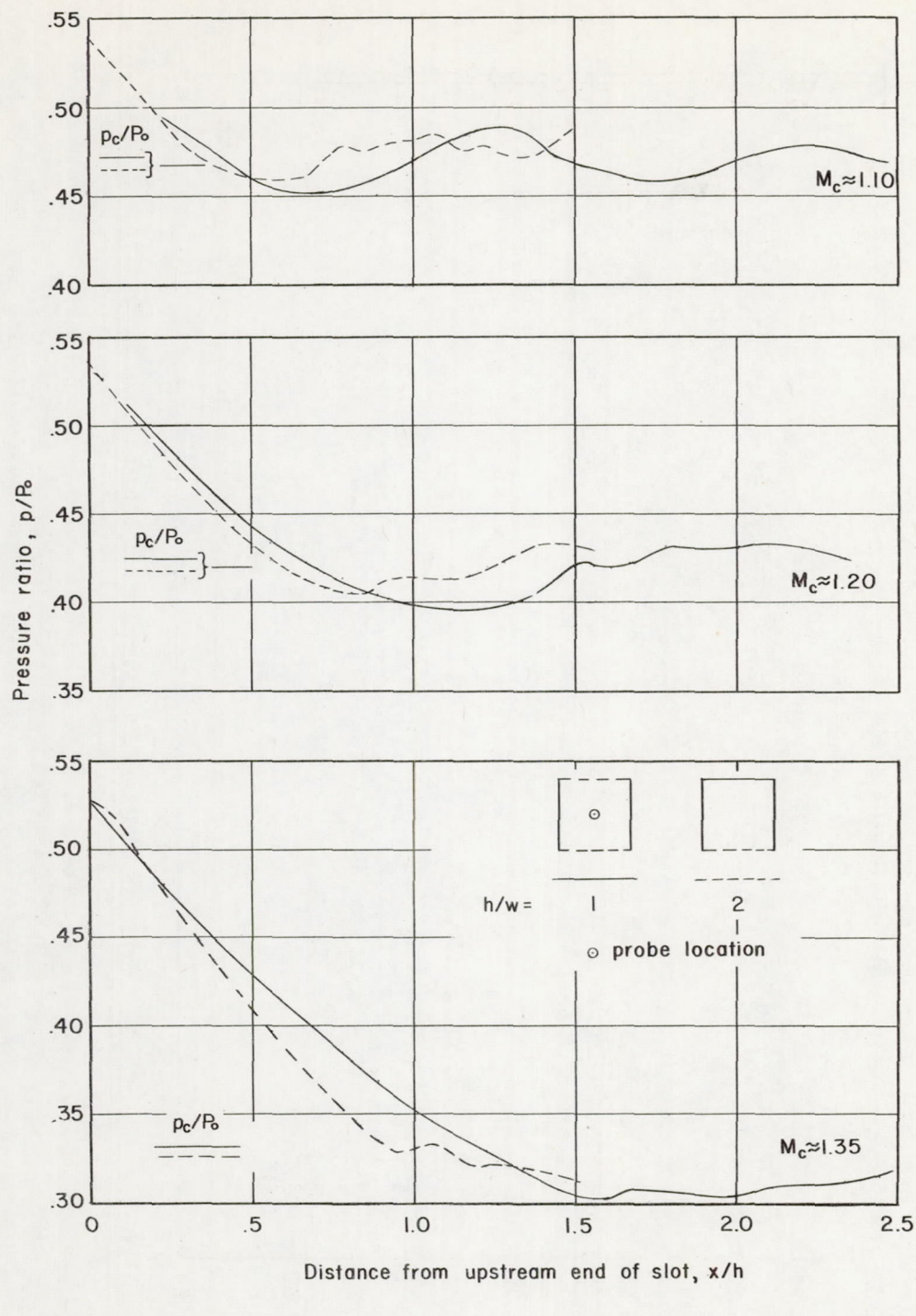(b) $\frac{nw_s}{w} = \frac{1}{5}$; $w_s = 0.225$ inch; $\Phi = 2.75°$; taper = 0.045 to 0.225 inch.
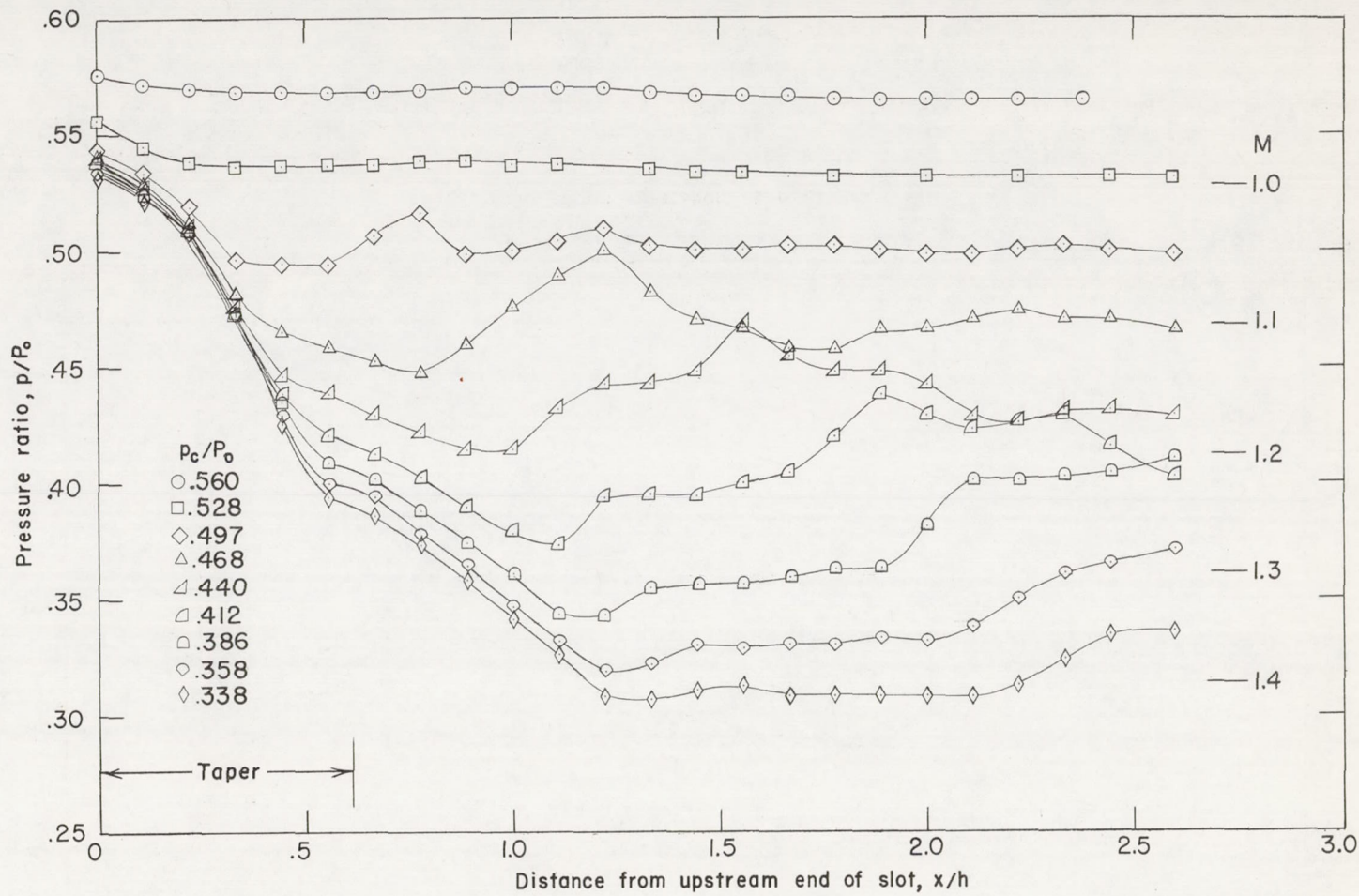
Figure 4.- Continued.

(c) $\dfrac{nw_s}{w} = \dfrac{1}{5}$; $w_s = 0.225$ inch; $\Phi = 2.75^\circ$; taper = 0.094 to 0.225 inch.
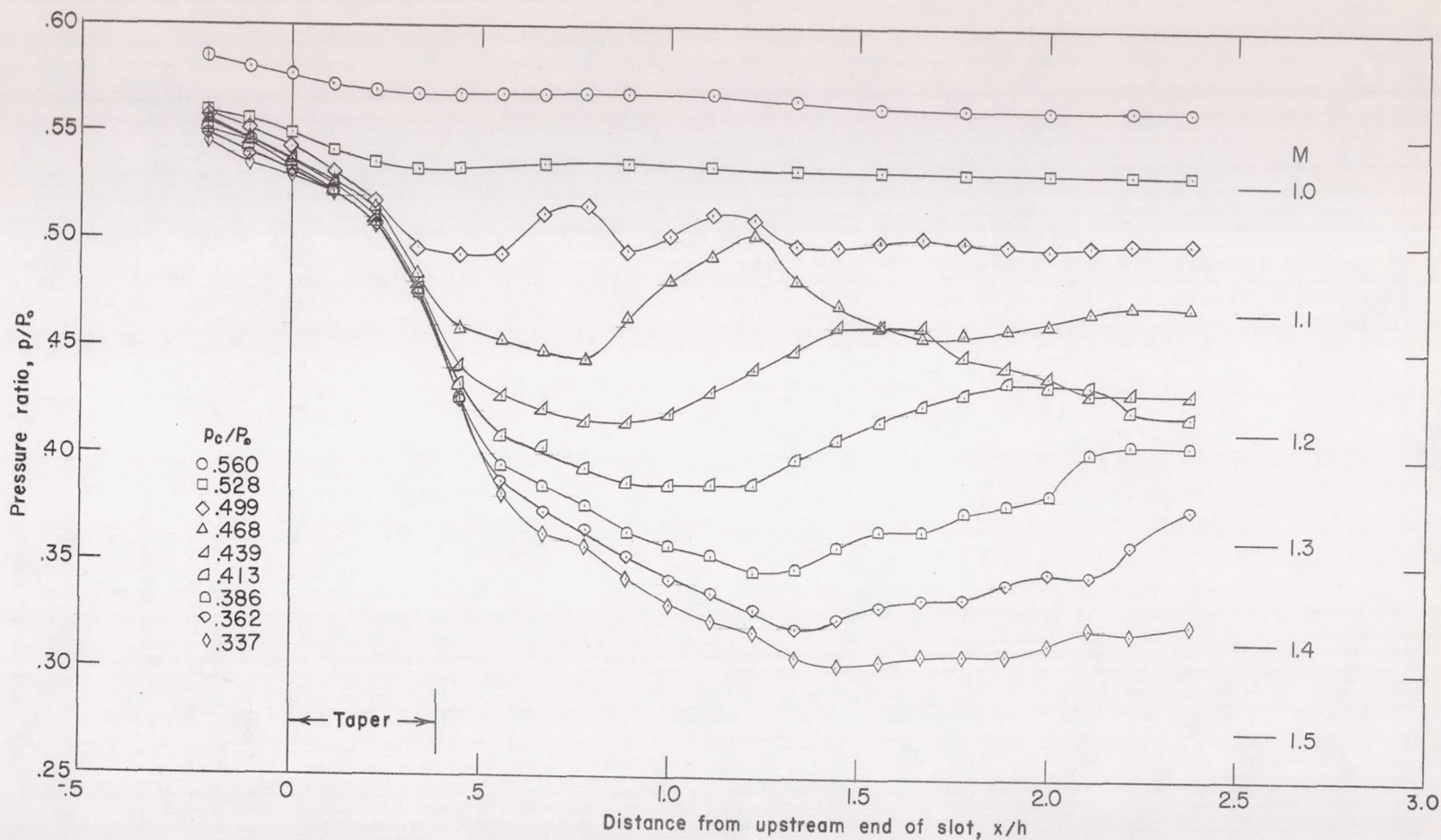
Figure 4.- Continued.

(d) $\frac{nw_s}{w} = \frac{1}{5}$; $w_s = 0.225$ inch; $\Phi = 2.75°$; taper = 0.141 to 0.225 inch.
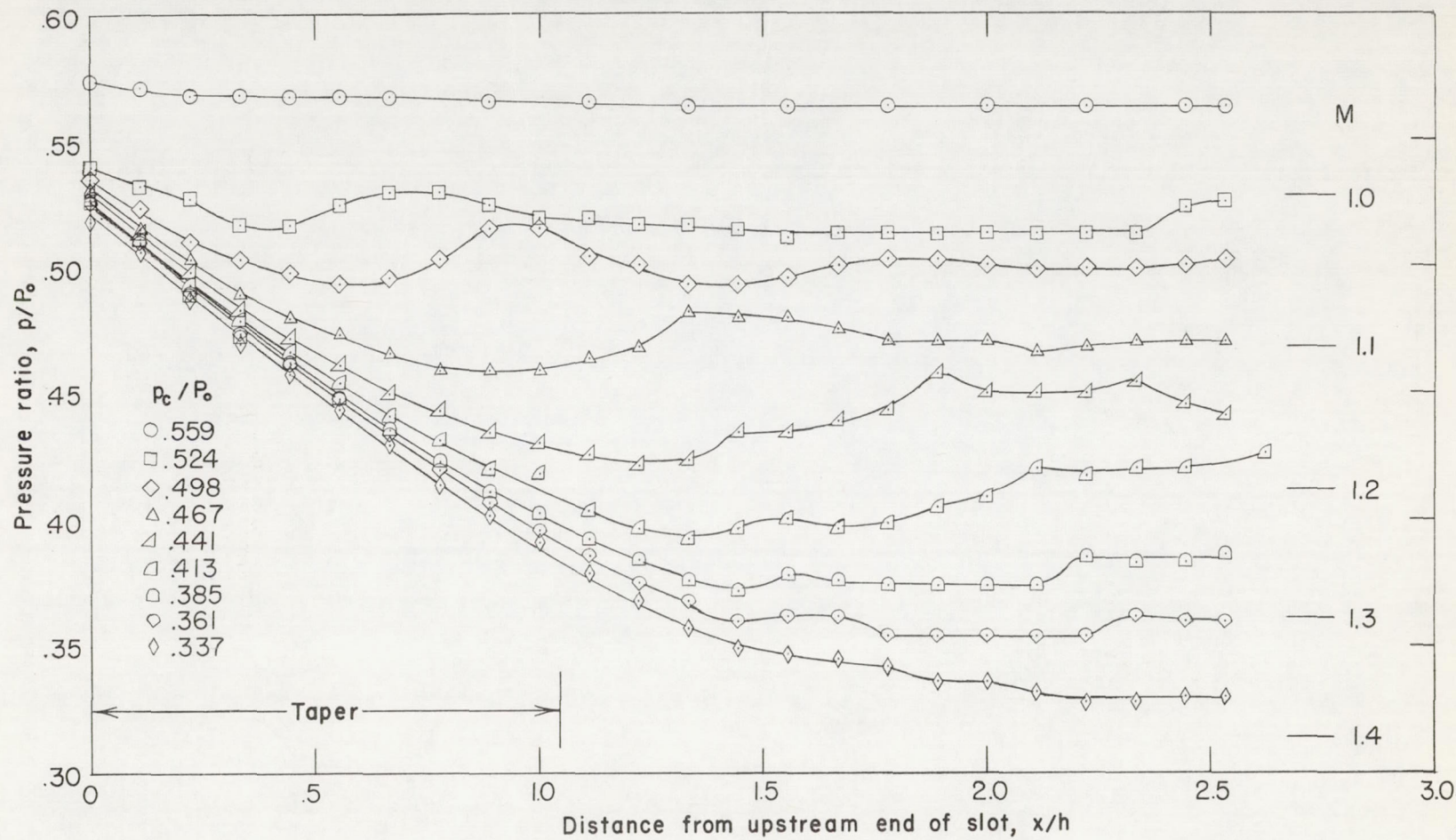
Figure 4.- Continued.

(e) $\dfrac{n w_s}{w} = \dfrac{1}{10}$; $w_s = 0.113$ inch; $\Phi = 1.38^\circ$.

Figure 4.- Continued.
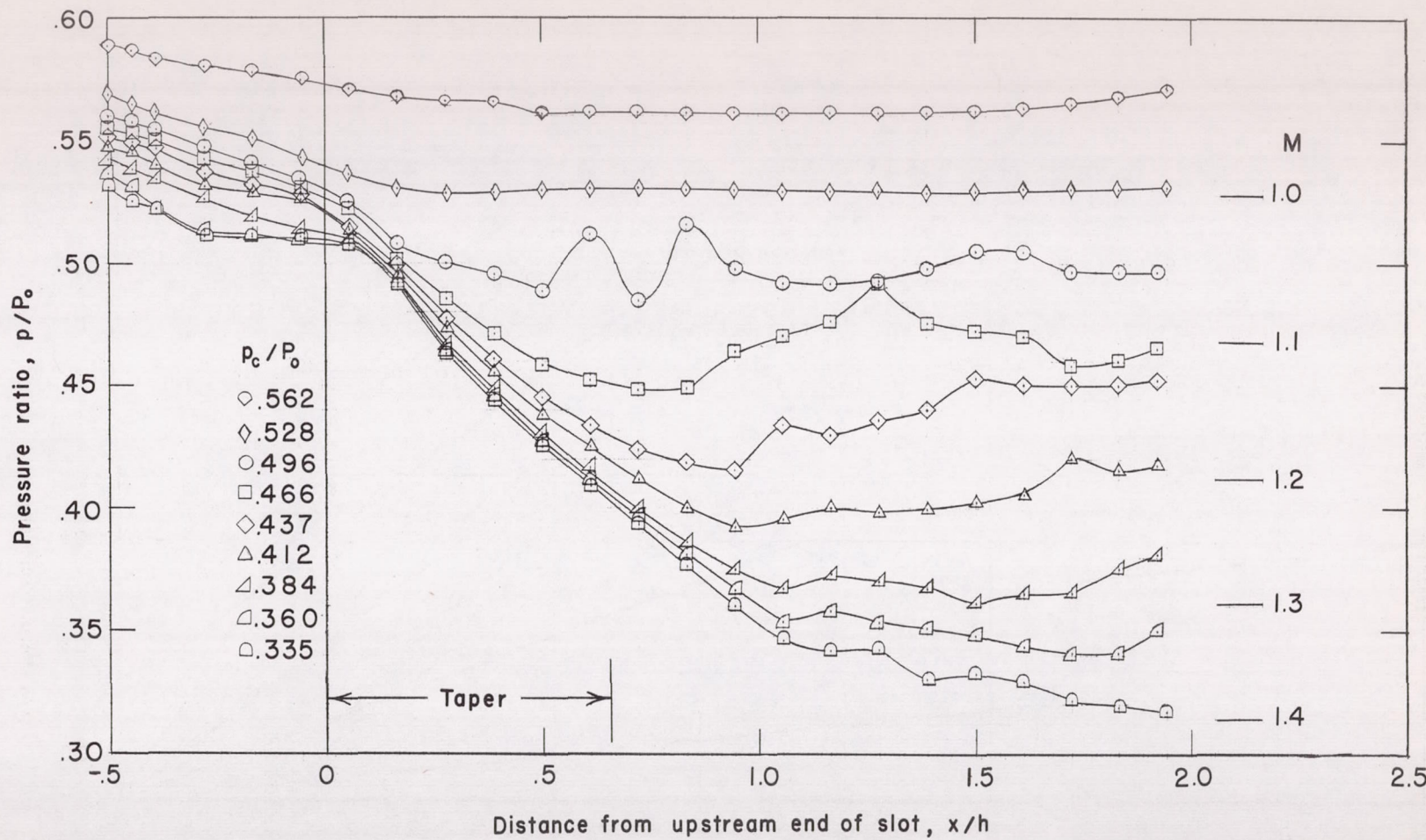
(f) $\dfrac{nw_s}{w} = \dfrac{1}{8}$; $w_s = 0.141$ inch; $\Phi = 2.75^\circ$.

Figure 4.- Continued.
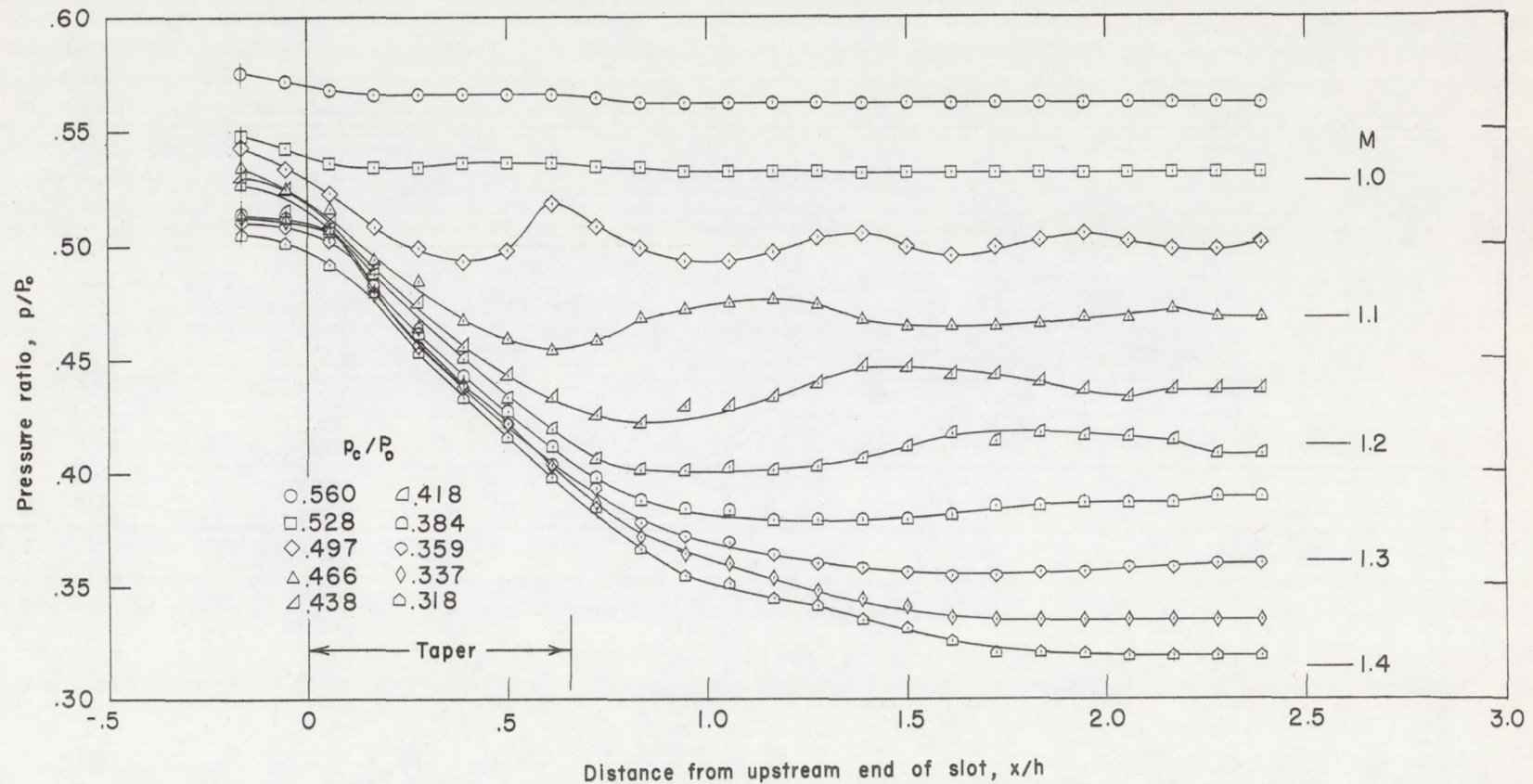
(g) $\dfrac{nw_s}{w} = \dfrac{1}{8}$; $w_s = 0.141$ inch; $\Phi = 2.75^\circ$; variable depth along taper.

Figure 4.- Continued.
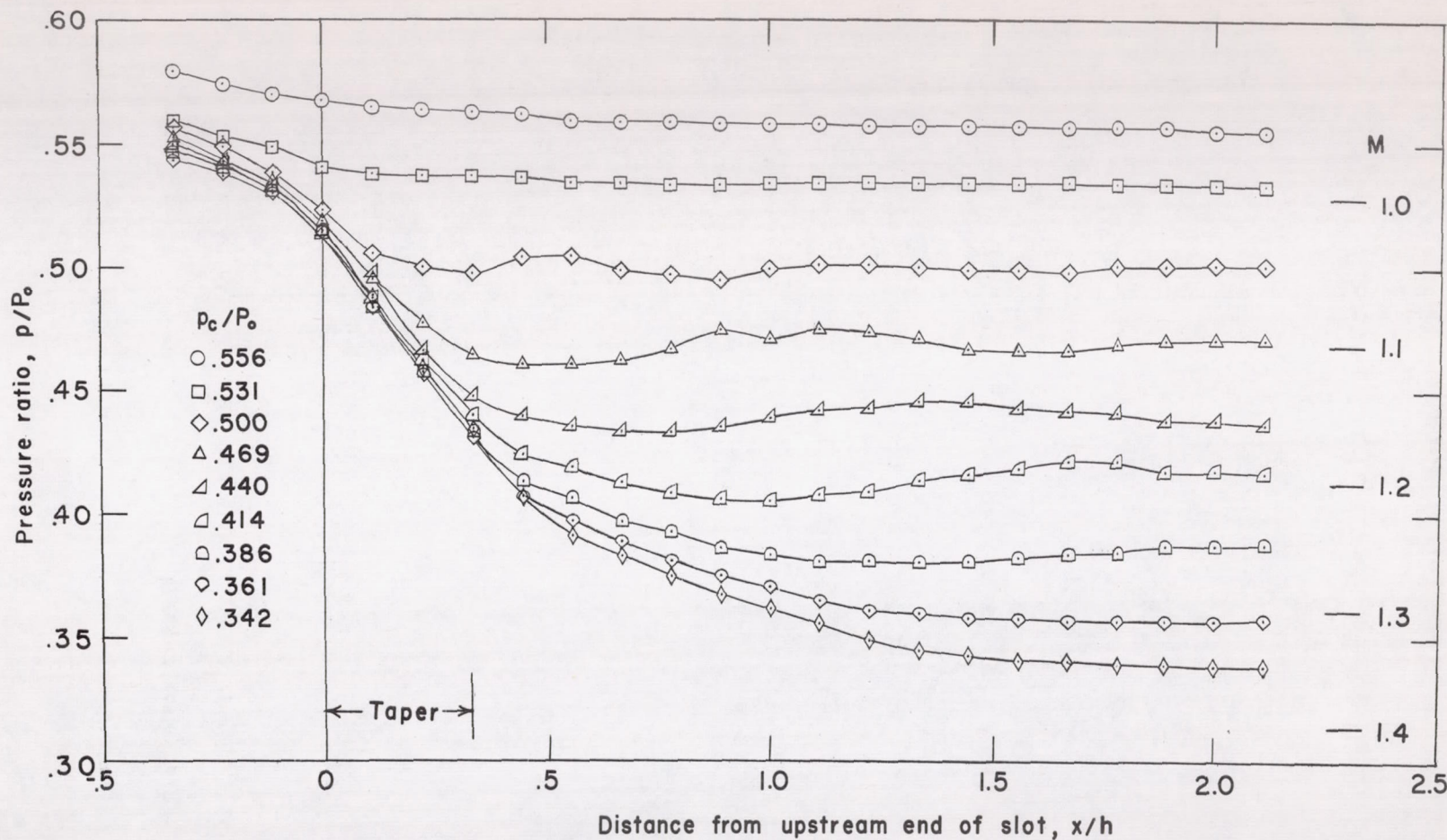
(h) $\dfrac{nw_s}{w} = \dfrac{1}{8}$; $w_s = 0.141$ inch; $\Phi = 5.50°$; variable depth along taper.

Figure 4.- Concluded.
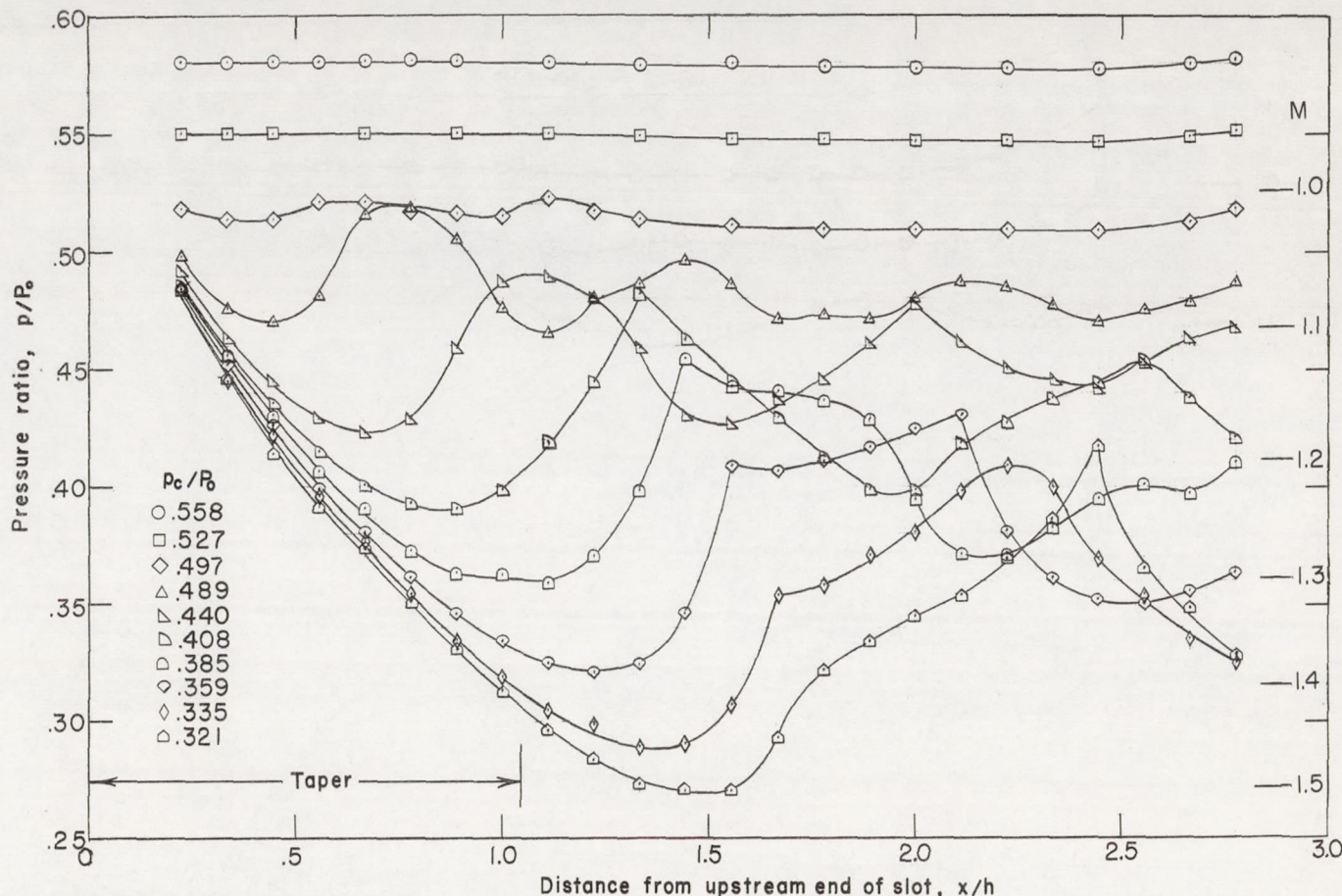
(a) $\dfrac{nw_s}{w} = \dfrac{1}{5}$; $w_s = 0.225$ inch; $\Phi = 2.75°$.

Figure 5.- Pressure distribution along center line (four walls slotted);
$w = 4\dfrac{1}{2}$ inches; $h = 4\dfrac{1}{2}$ inches.
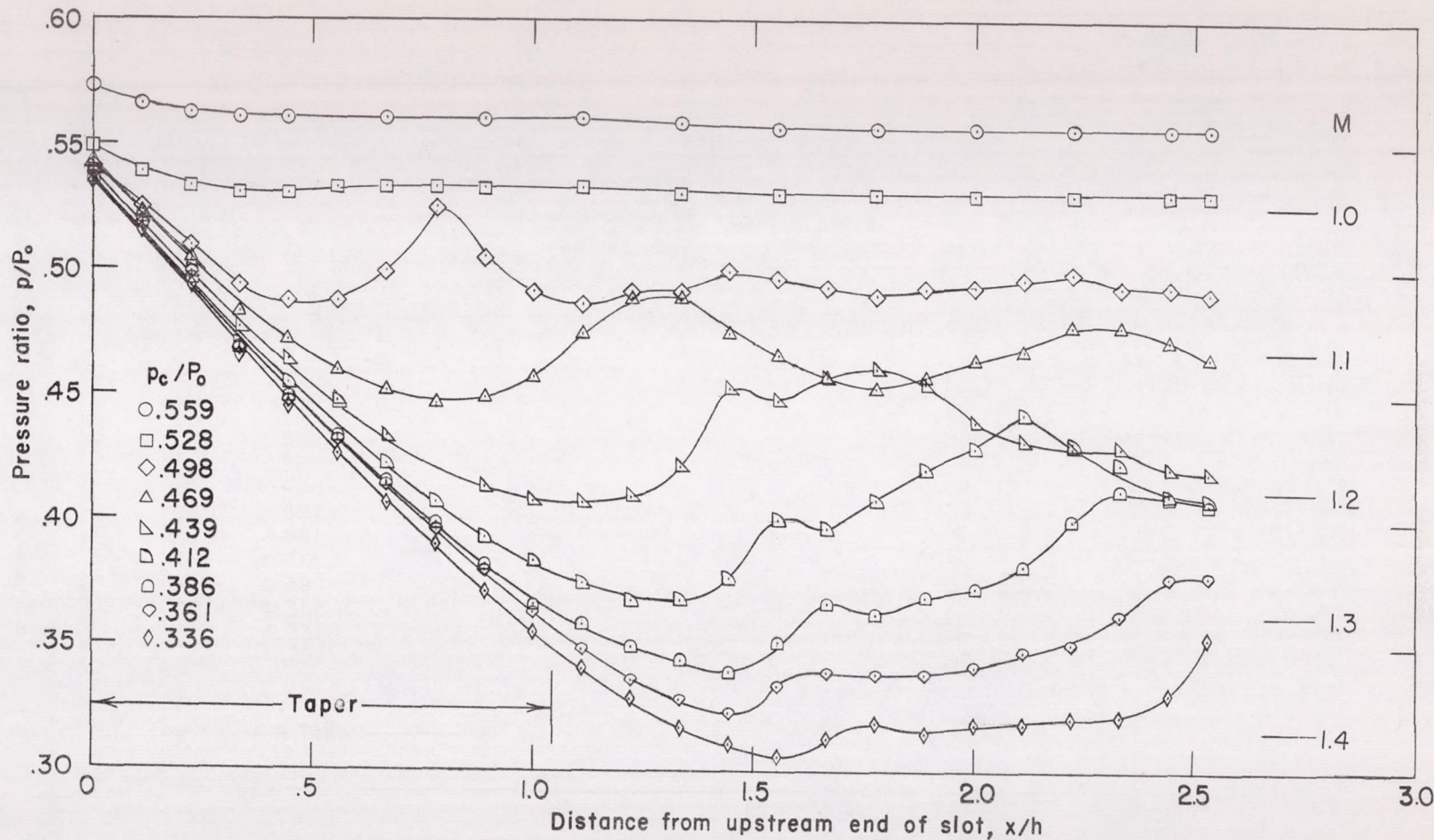
(b) $\dfrac{nw_s}{w} = \dfrac{1}{10}$; $w_s = 0.113$ inch; $\Phi = 1.38°$.

Figure 5.- Concluded.
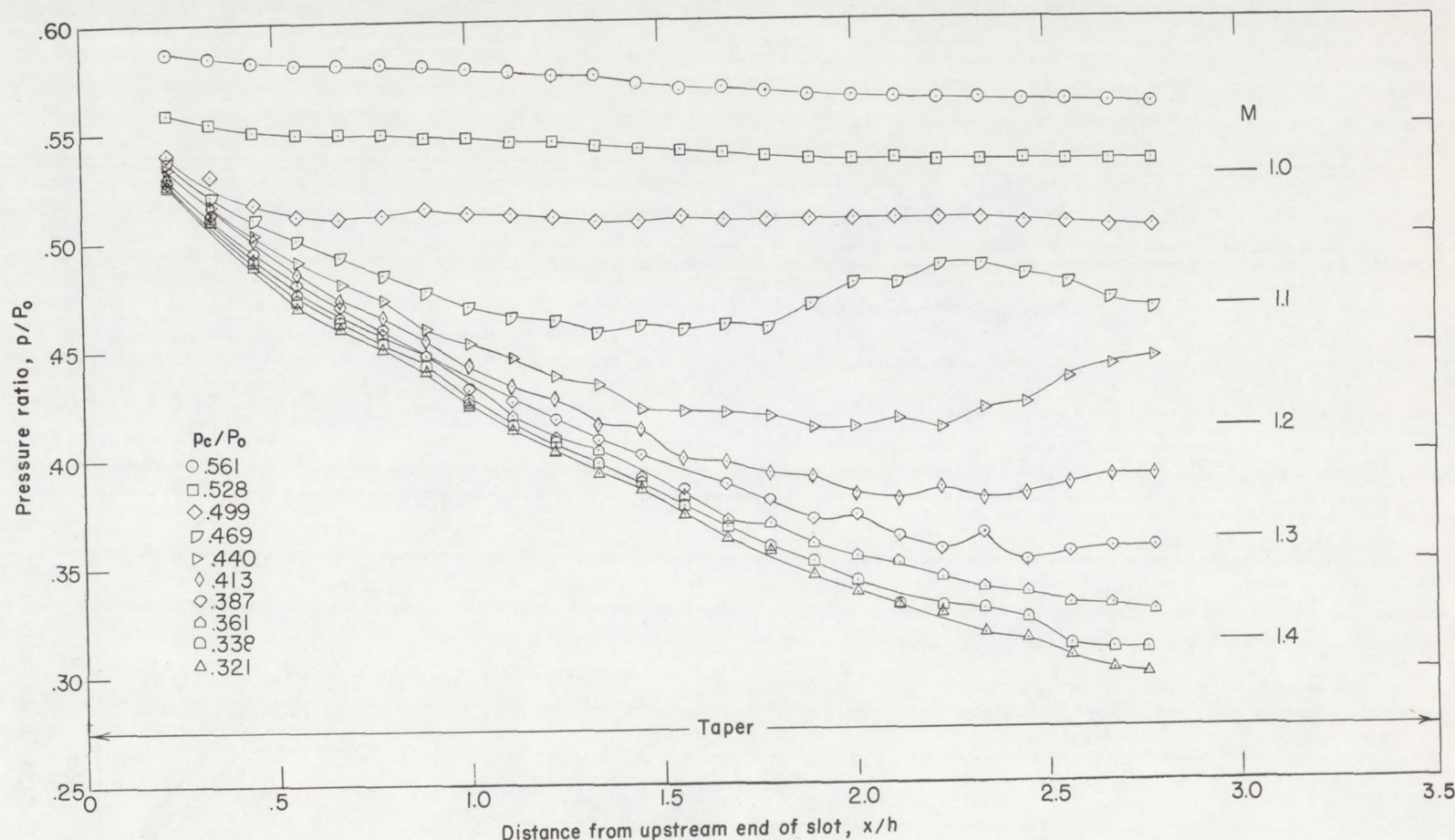
(a) $\dfrac{nw_s}{w} = \dfrac{1}{10}$; $w_s = 0.432$ inch; $\Phi = 1.46^{\circ}$.

Figure 6.- Pressure distribution along center line of slotted corner configuration; $w = 4\frac{1}{2}$ inches; $h = 4\frac{1}{2}$ inches.
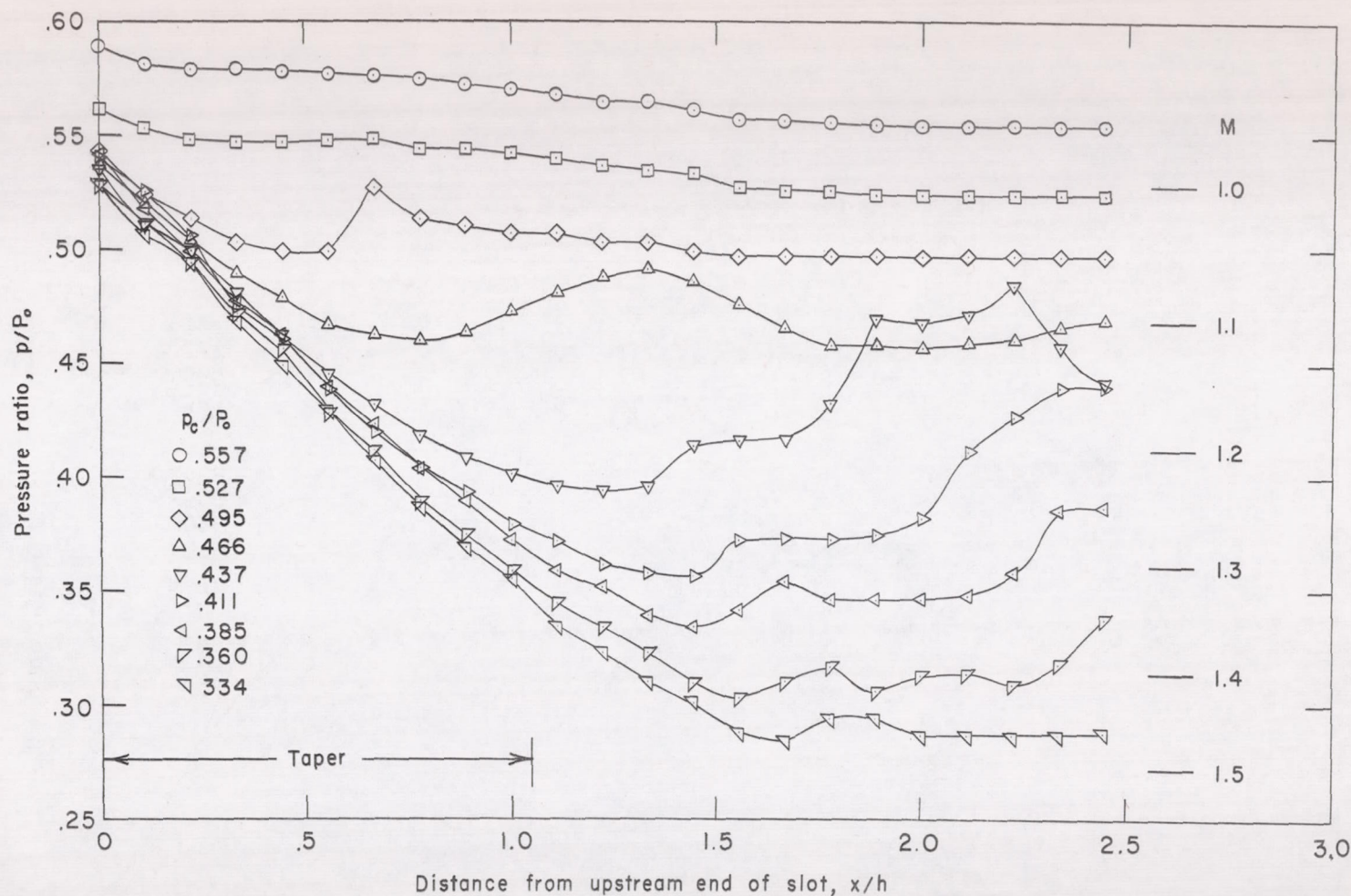
(b) $\dfrac{nw_s}{w} = \dfrac{1}{10}$; $w_s = 0.432$ inch; $\Phi = 5.24°$.

Figure 6.- Continued.
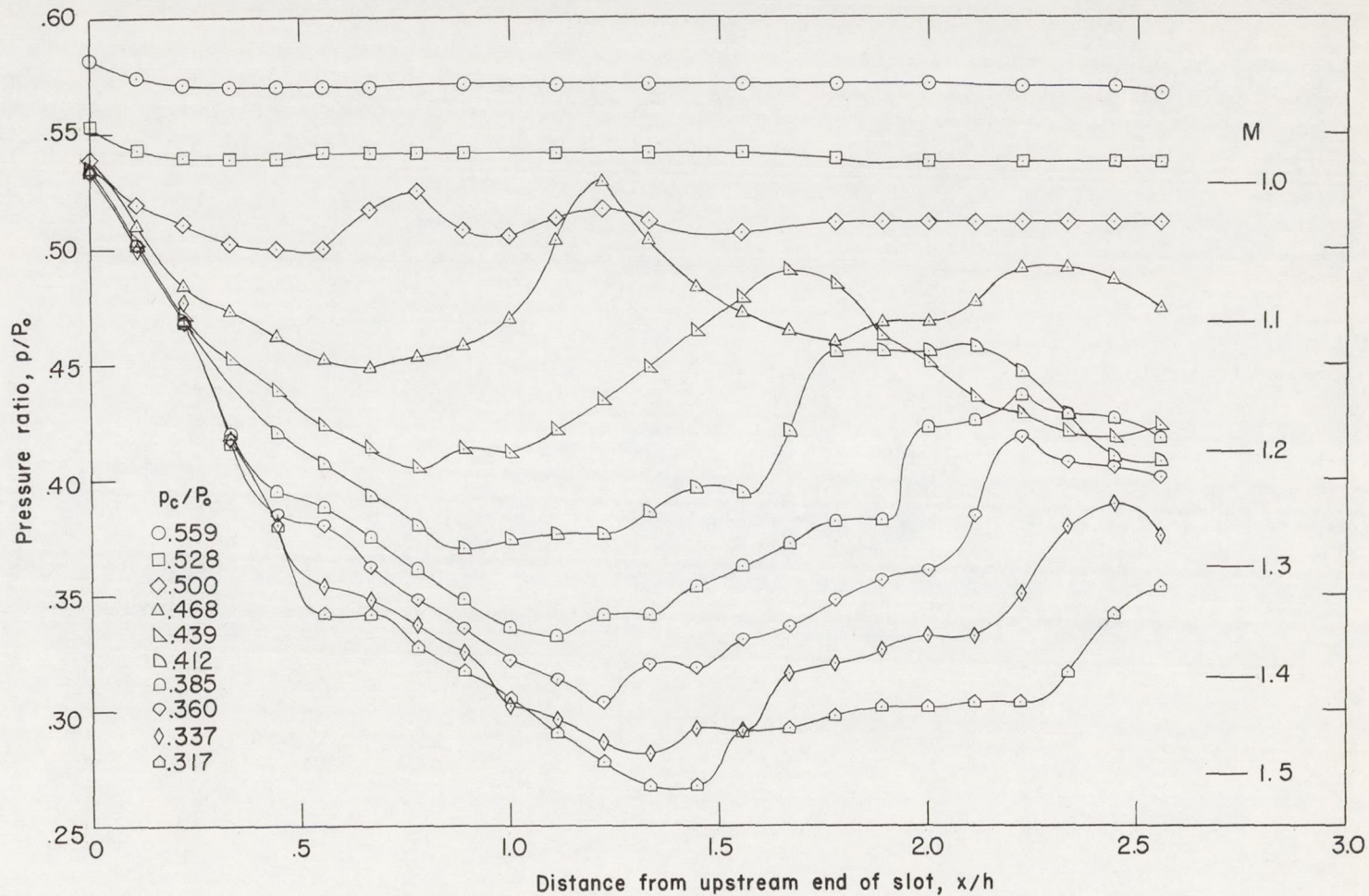
(c) $\dfrac{nw_s}{w} = \dfrac{1}{8}$; $w_s = 0.540$ inch; $\Phi = 180°$.

Figure 6.- Continued.
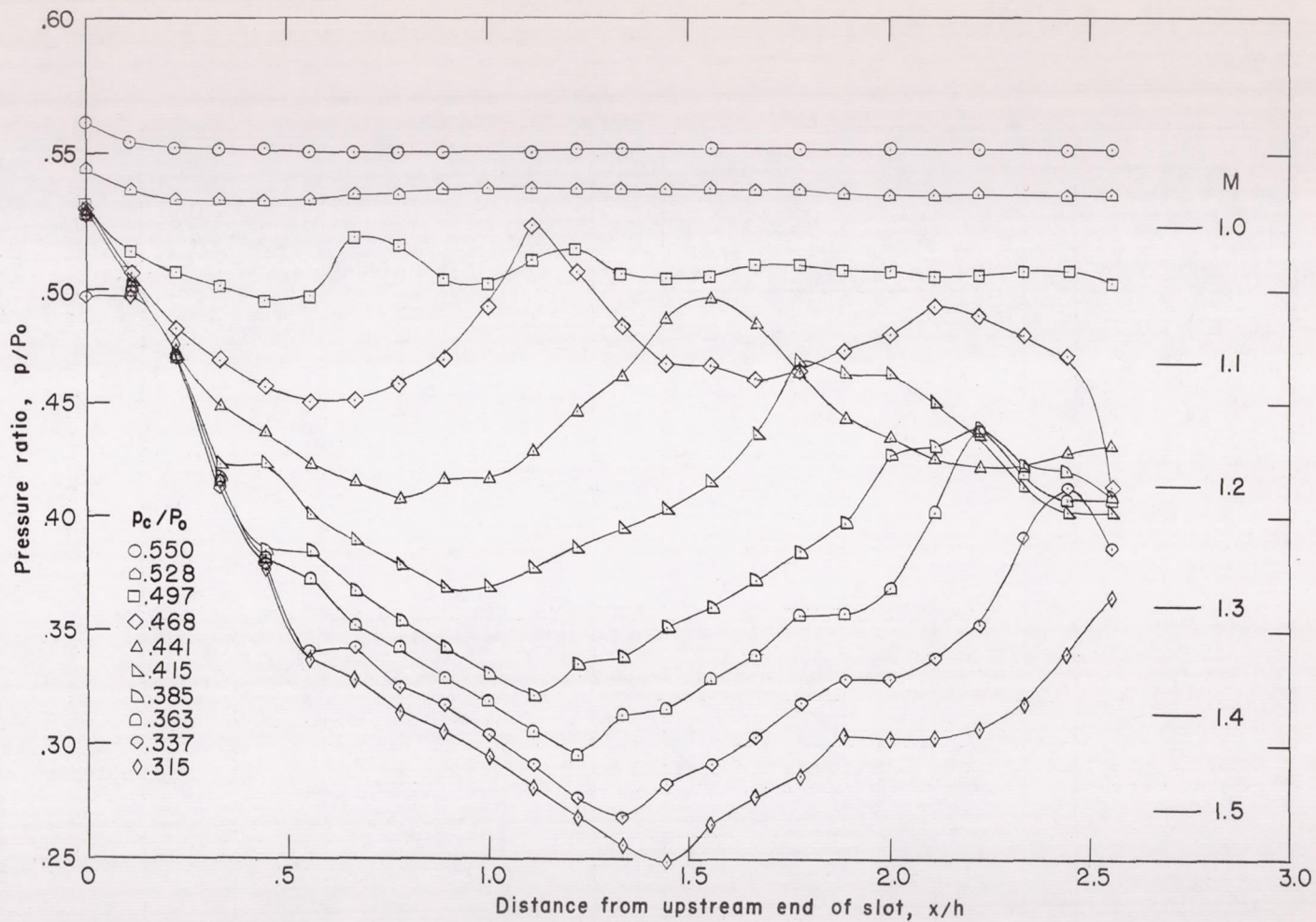
(d) $\dfrac{nw_s}{w} = \dfrac{1}{10}$; $w_s = 0.432$ inch; $\Phi = 180°$.

Figure 6.- Concluded.

.55

.50

p_c/P_0
}

.45

$M_c \approx 1.10$

.40

.55

.50

p_c/P_0
}

Pressure ratio, p/P_0

.45

.40

$M_c \approx 1.20$

.35

.55

.50

.45

h/w =   1   2

.40

o probe location

.35

p_c/P_0

$M_c \approx 1.35$

.30

0   .5   1.0   1.5   2.0   2.5

Distance from upstream end of slot, x/h

(a) Effect of tunnel height to width ratio, $\dfrac{n w_s}{w} = \dfrac{1}{5}$;

$w_s = 0.225$ inch; $\Phi = 2.75^{\circ}$.

Figure 7.- Comparisons of center-line pressure distribution.
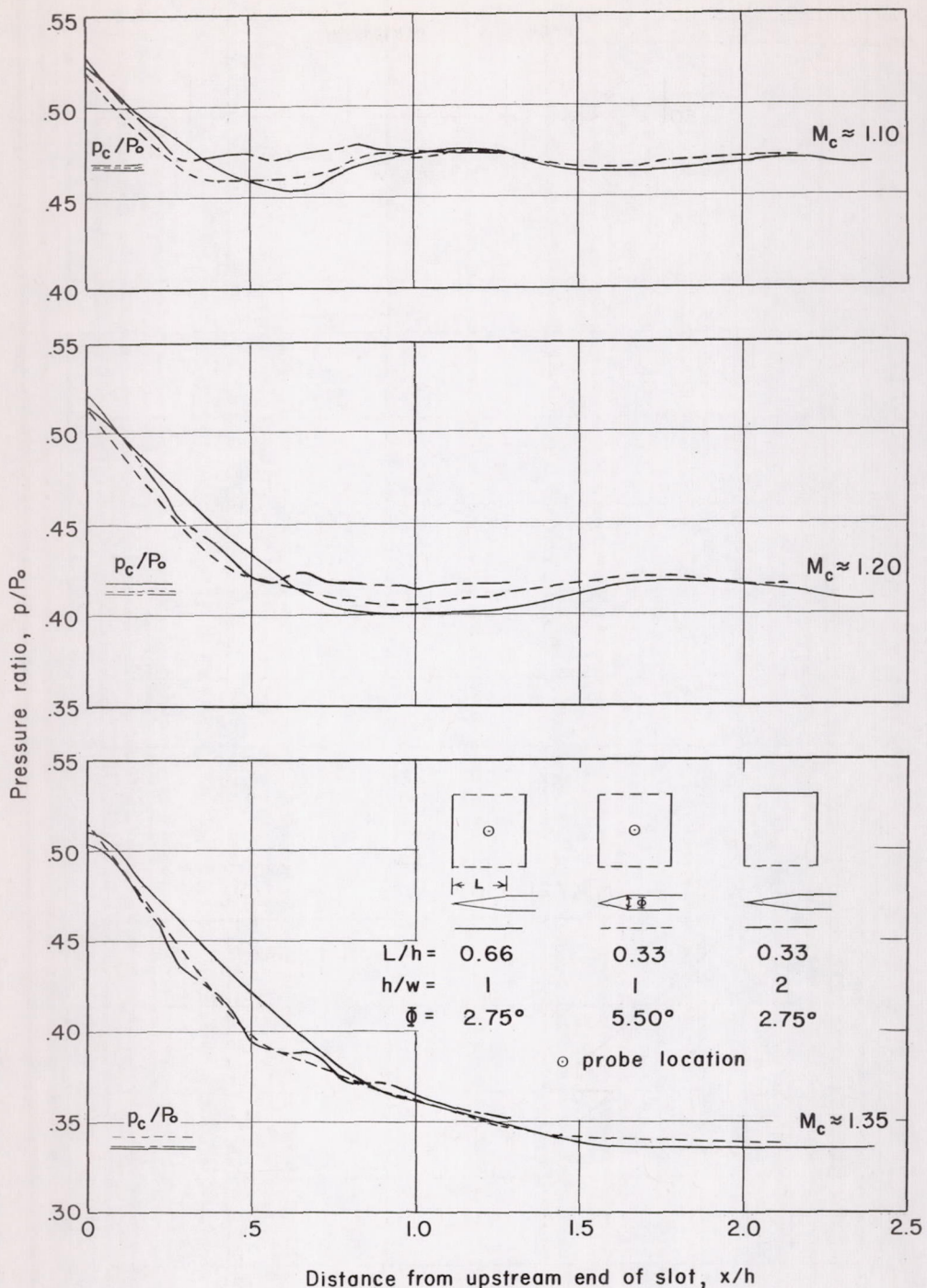
(b) Effect of slot taper length; $\dfrac{n w_s}{w} = \dfrac{1}{8}$; $w_s = 0.141$ inch.

Figure 7.- Continued.
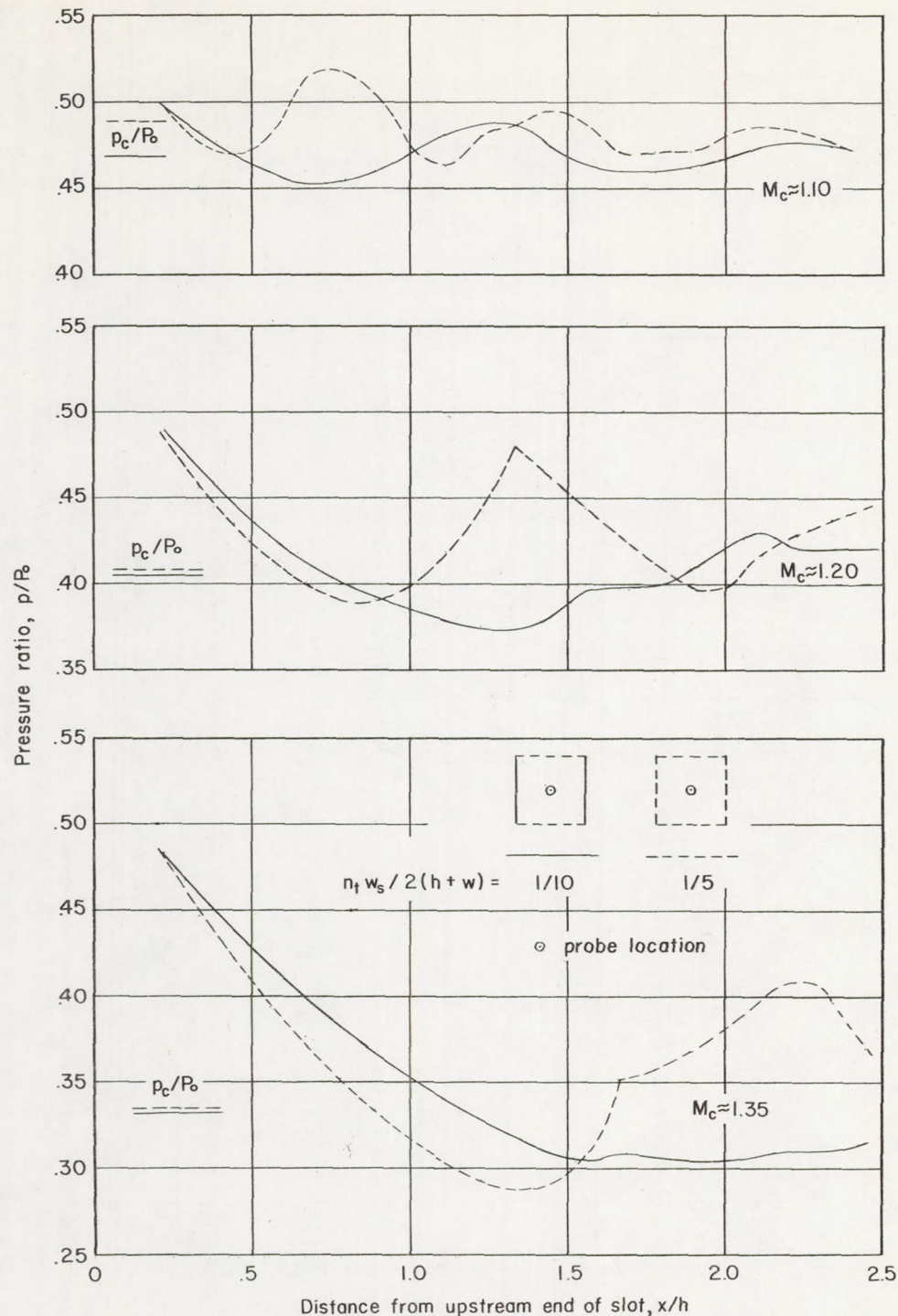
(c) Effect of slot location, $\dfrac{nw_s}{w} = \dfrac{1}{5}$; $w_s = 0.225$ inch; $\Phi = 2.75°$.

Figure 7.- Continued.
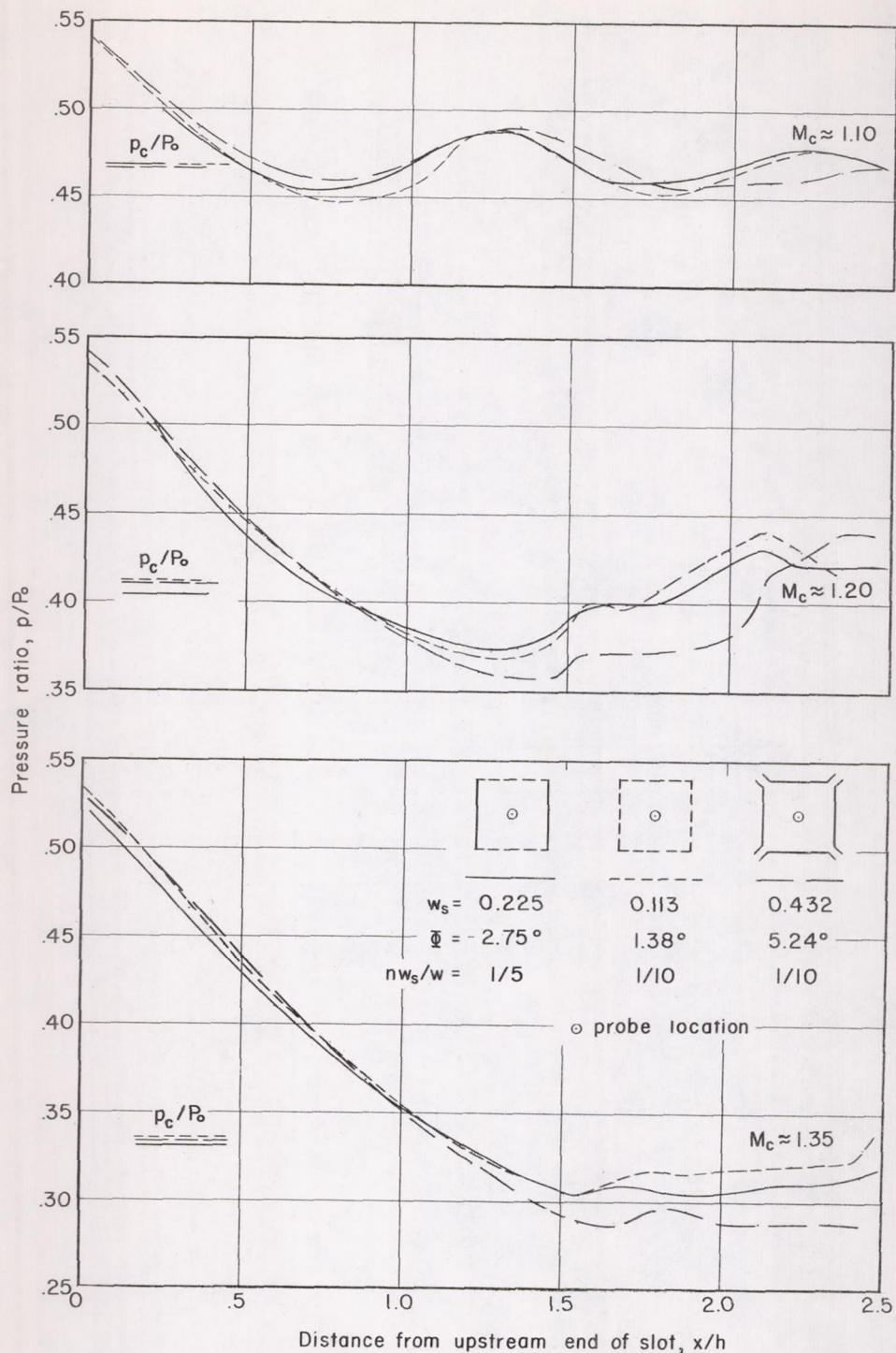
(d) Effect of total slot area to tunnel periphery ratio; $\dfrac{n_t w_s}{2(h + w)} = \dfrac{1}{10}$.
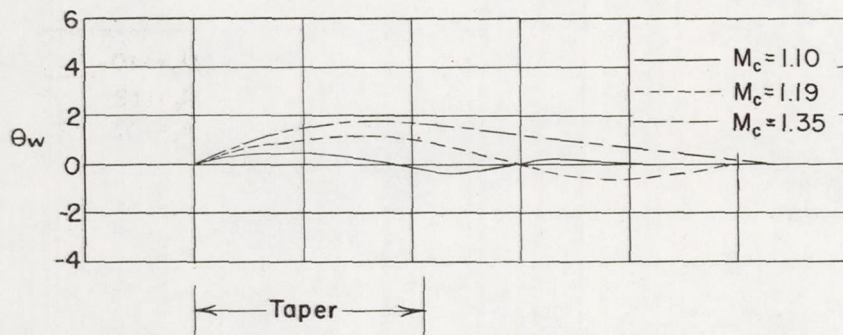
Figure 7.- Concluded.
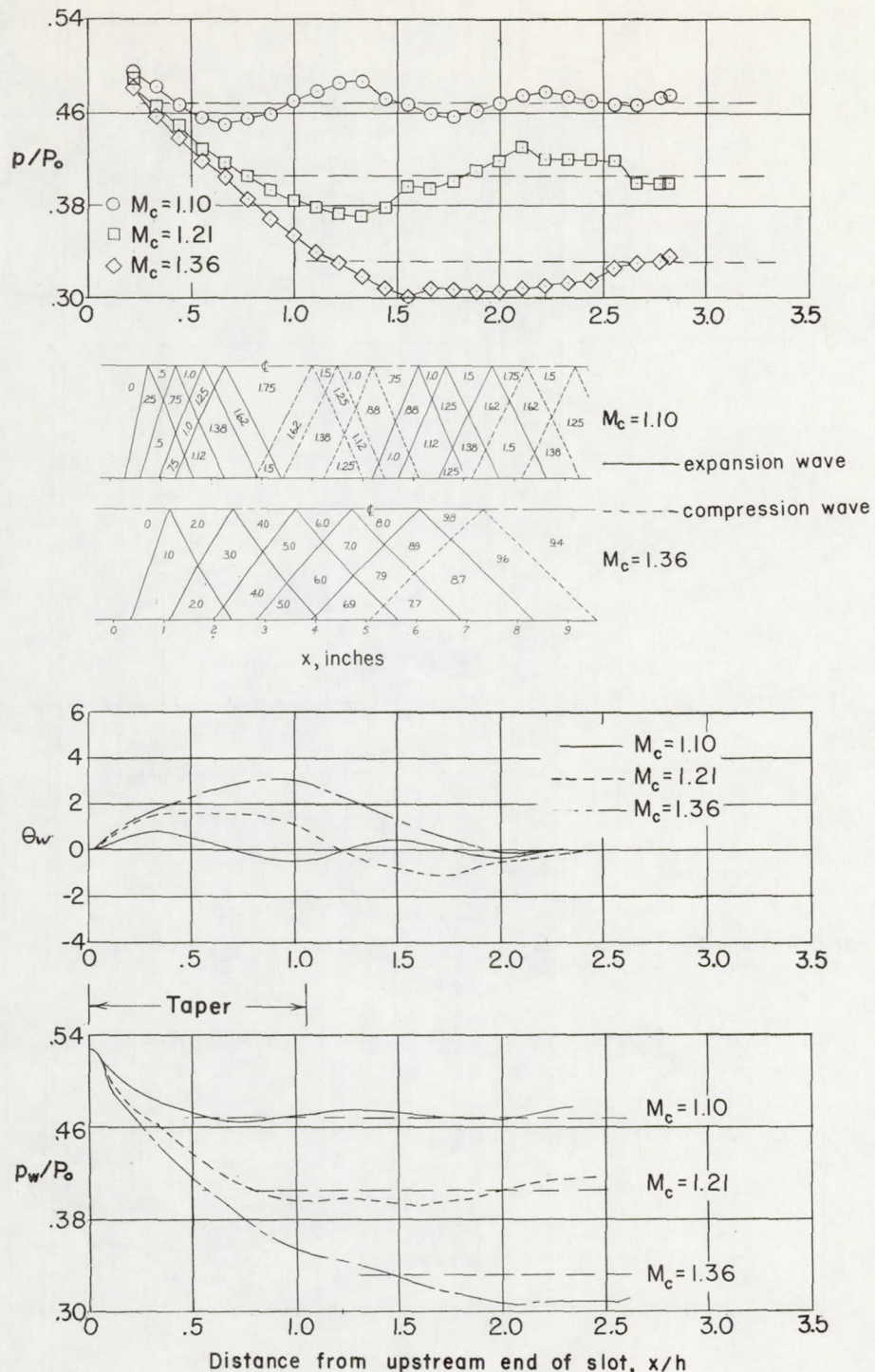
(a) $\dfrac{n w_s}{w} = \dfrac{1}{5}$; $w_s = 0.225$ inch; $\Phi = 2.75°$; taper = 0 to 0.225 inch.
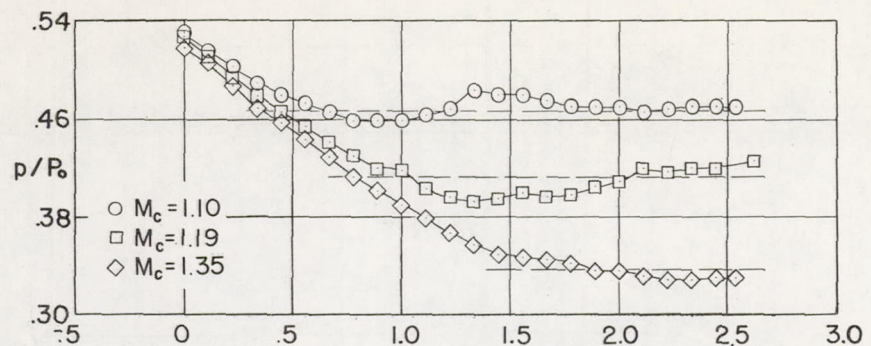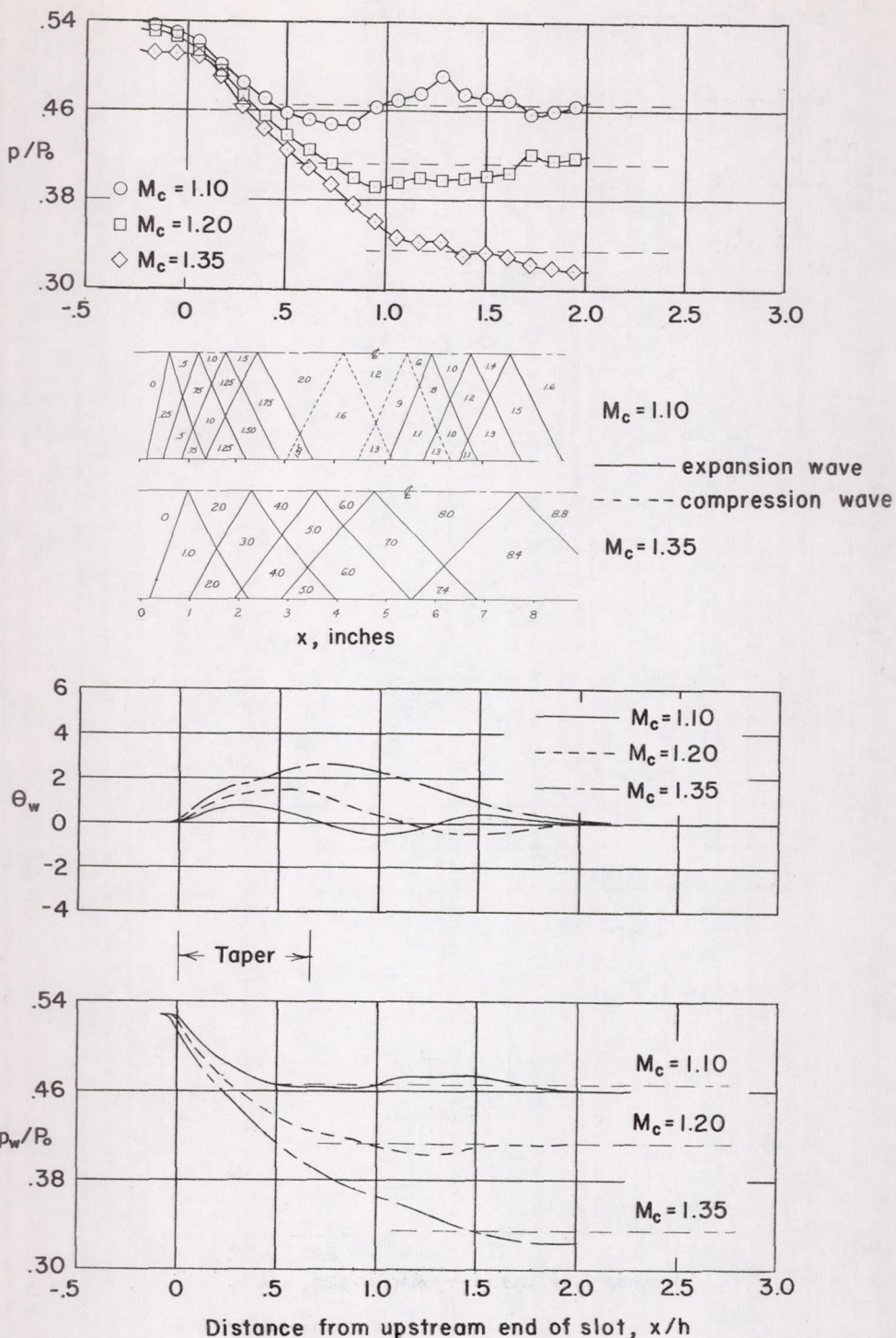
Figure 8.- Pressure and flow-angle distributions.
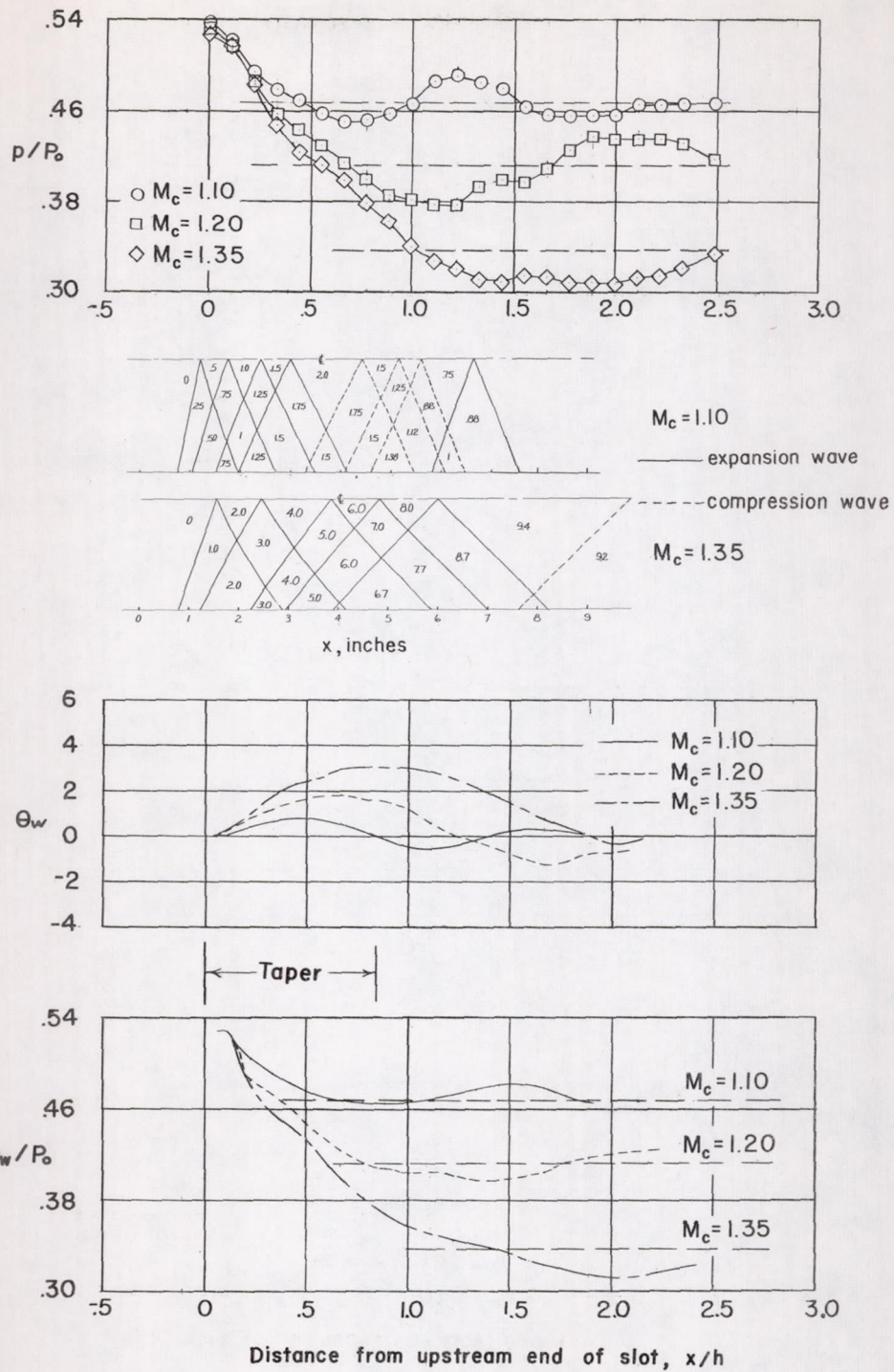
(b) $\dfrac{nw_s}{w} = \dfrac{1}{5}$; $w_s = 0.225$ inch; $\Phi = 2.75°$; taper = 0.045 to 0.225 inch.
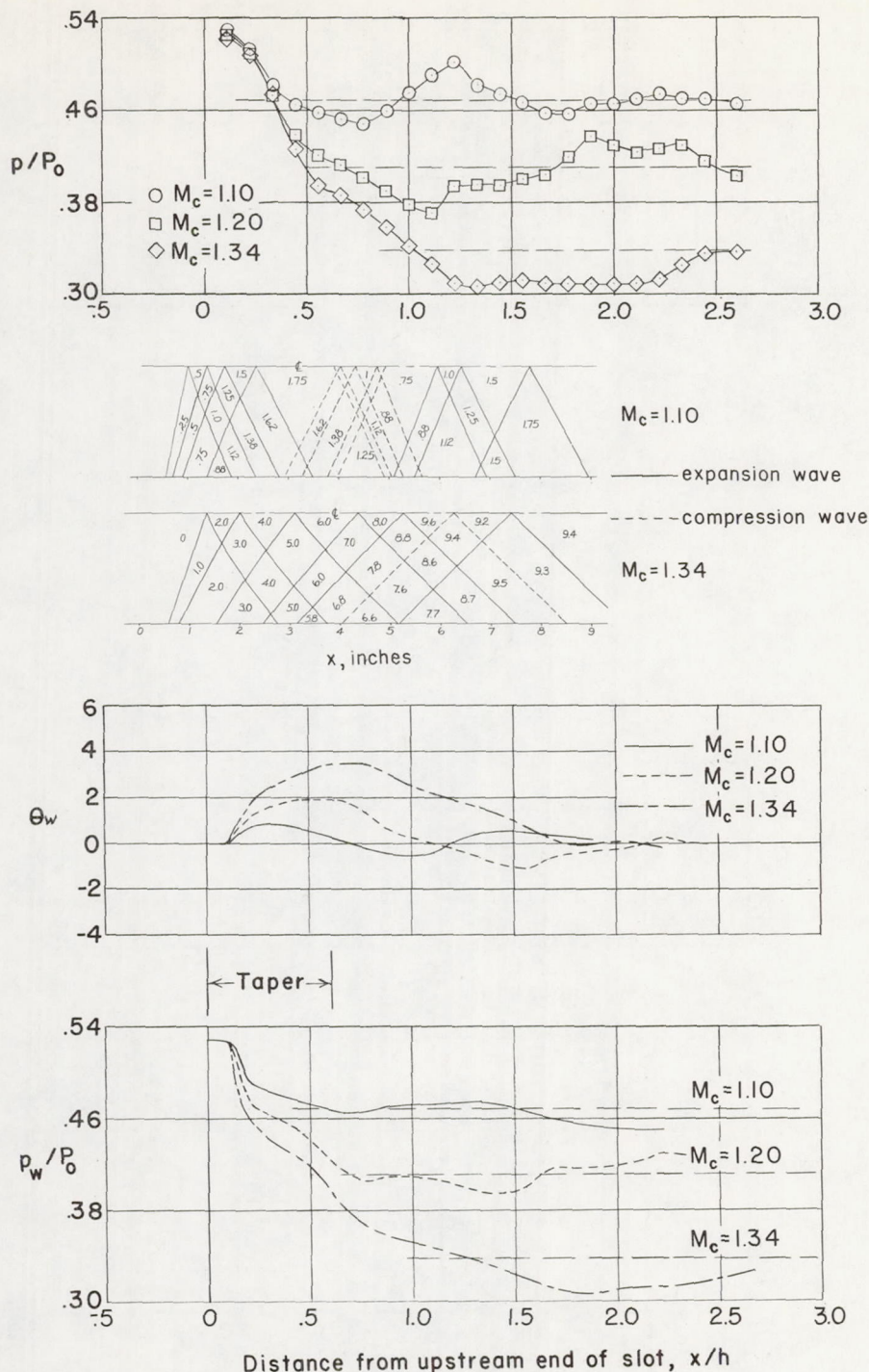
Figure 8.- Continued.

(c) $\dfrac{nw_s}{w} = \dfrac{1}{5}$; $w_s = 0.225$ inch; $\Phi = 2.75°$; taper = 0.094 to 0.225 inch.
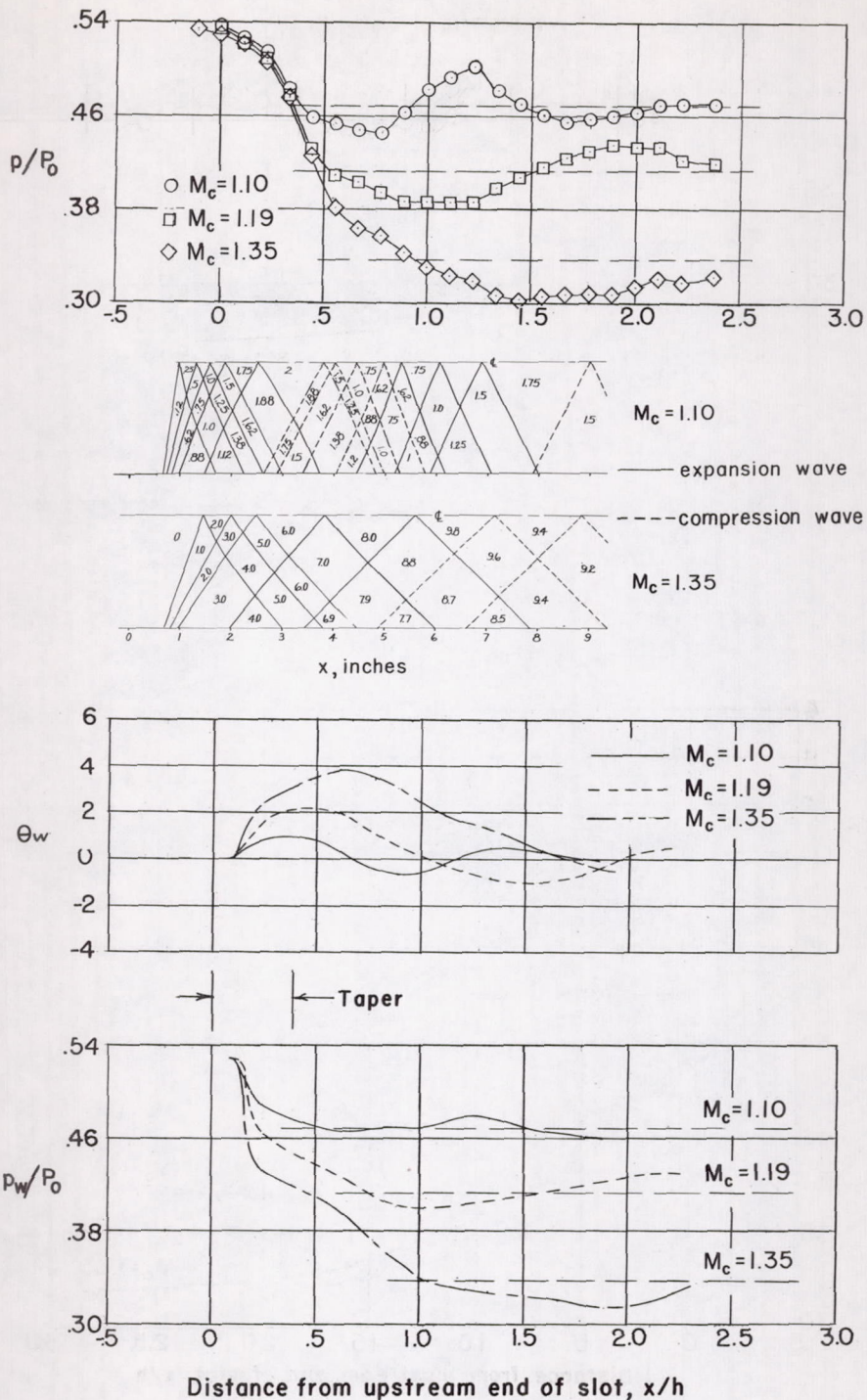
Figure 8.- Continued.

(d) $\dfrac{n w_S}{w} = \dfrac{1}{5}$; $w_S = 0.225$ inch; $\Phi = 2.75°$; taper $= 0.141$ to 0.225 inch.
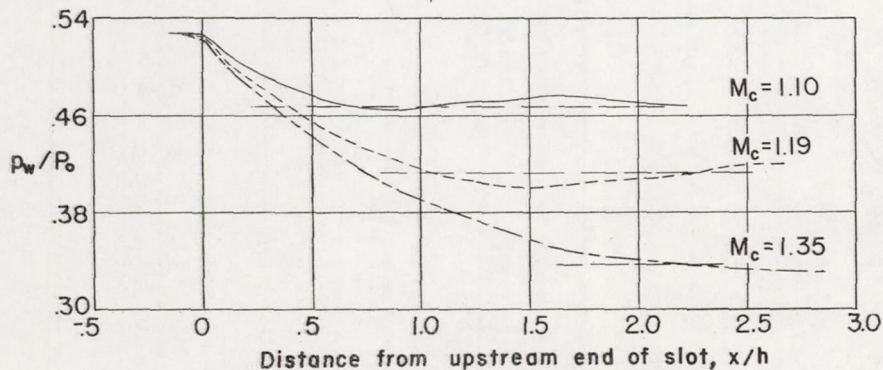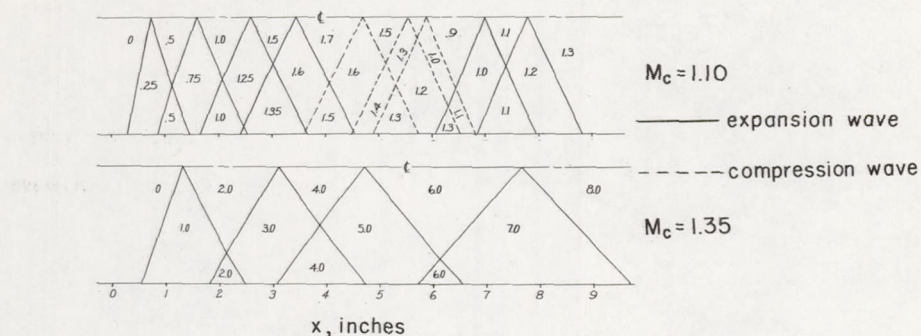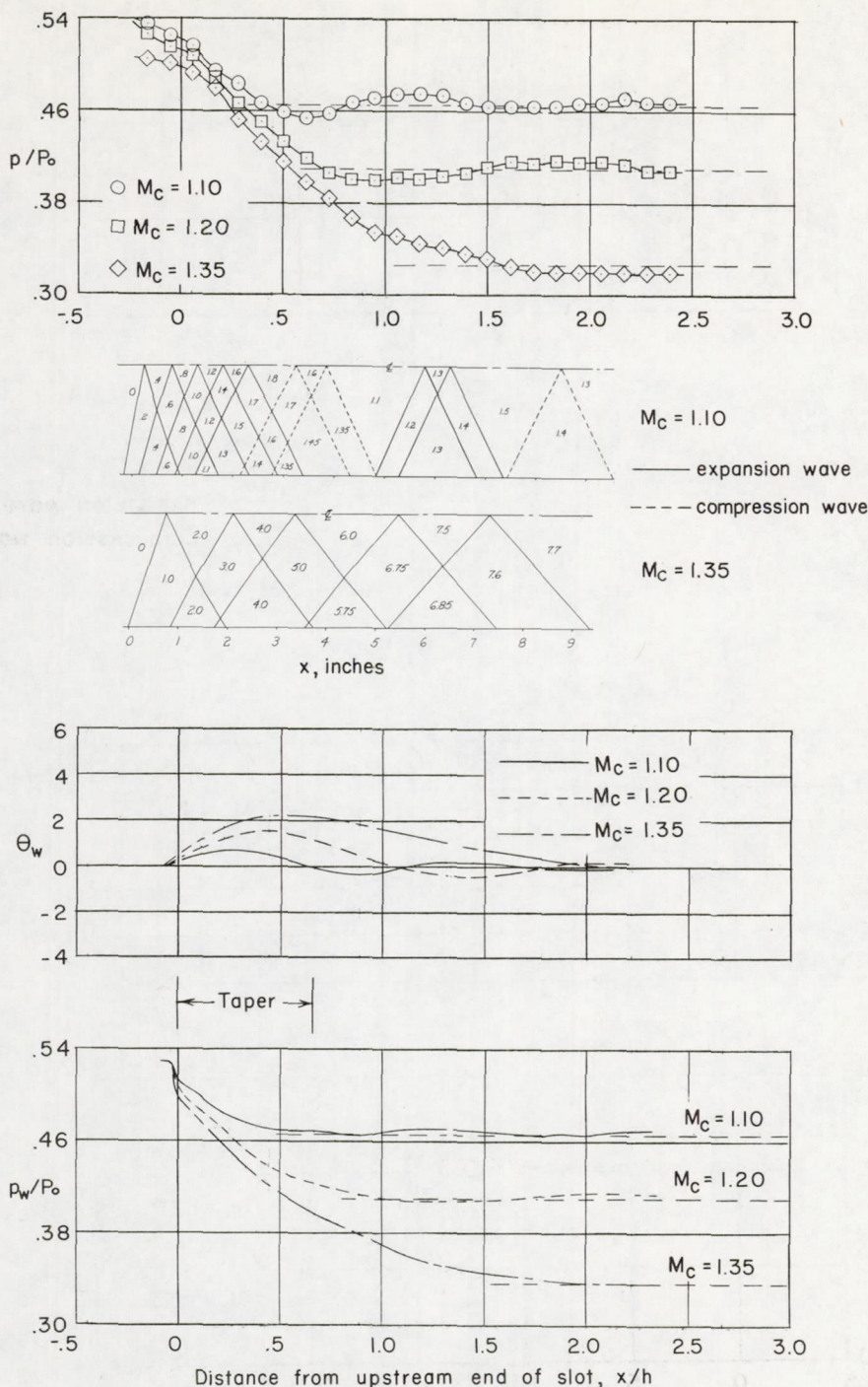
Figure 8.- Continued.
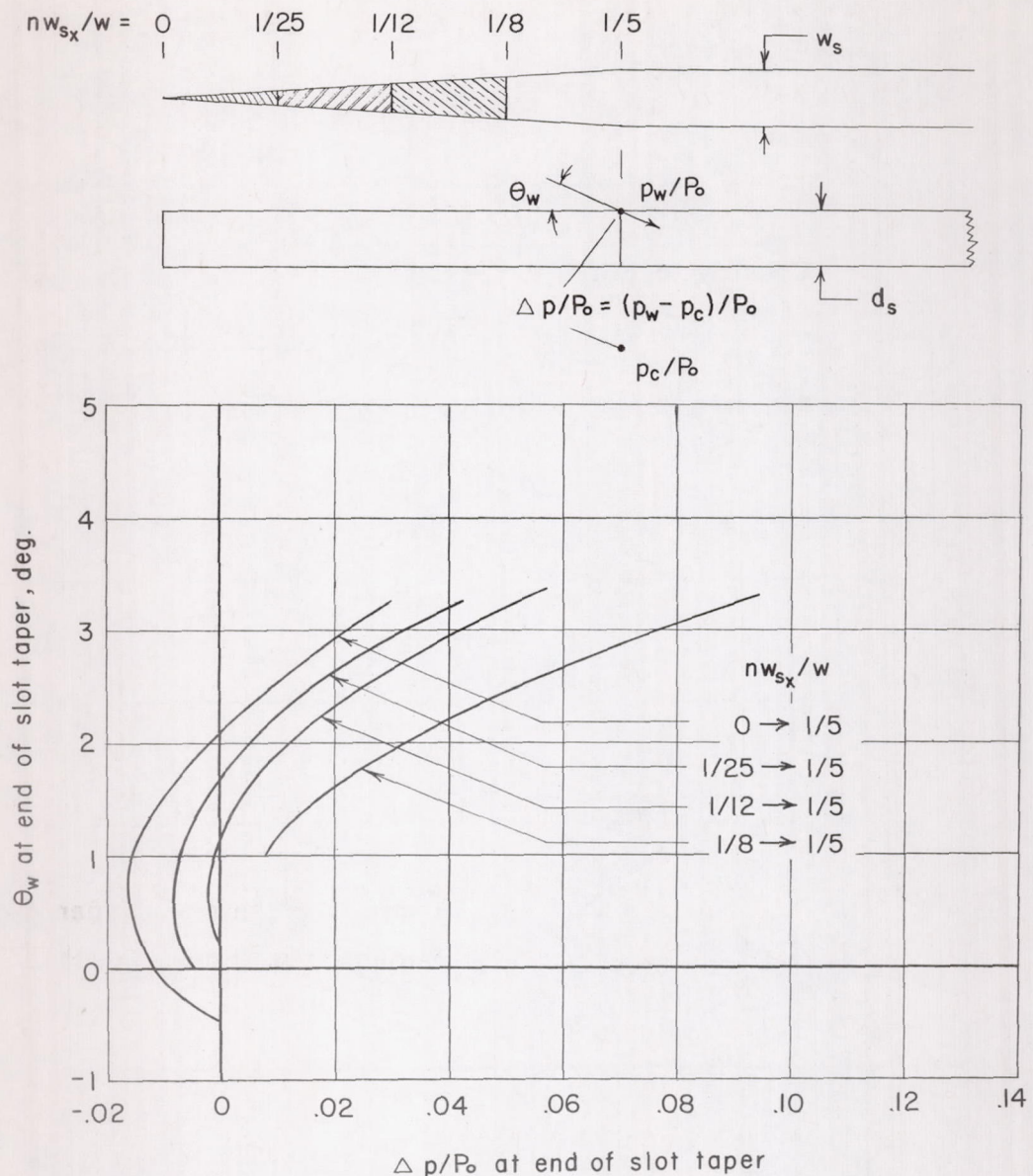
(e) $\dfrac{nw_S}{w} = \dfrac{1}{10}$; $w_S = 0.113$ inch; $\Phi = 1.38°$.

Figure 8.- Continued.

(f) $\dfrac{nw_s}{w} = \dfrac{1}{8}$; $w_s = 0.141$ inch; $\Phi = 2.75^\circ$.

Figure 8.- Continued.

(g) $\dfrac{nw_S}{w} = \dfrac{1}{8}$; $w_S = 0.141$ inch; $\Phi = 2.75^{\circ}$; slot depth varies from 1/2 to 1/16 inch along taper.
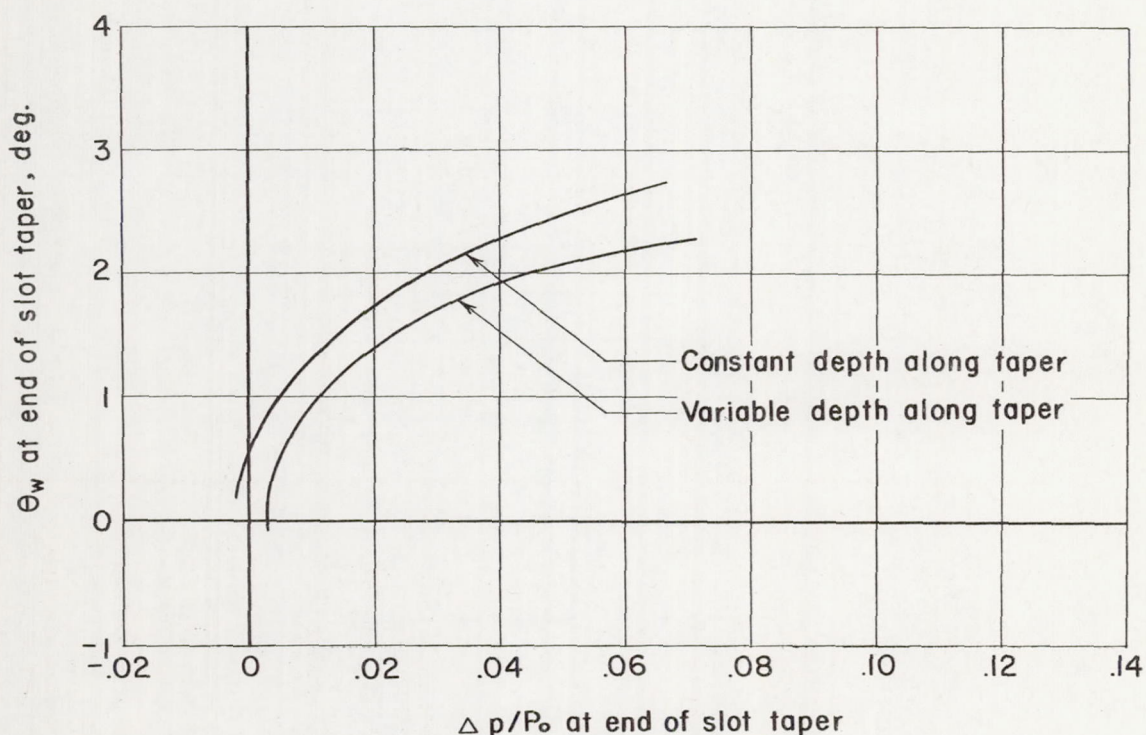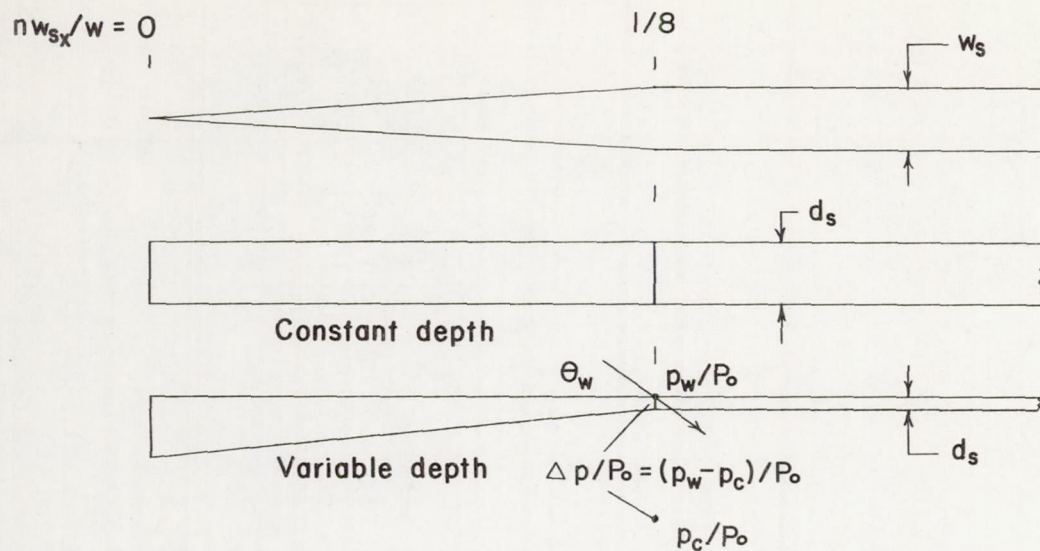
Figure 8.- Concluded.

(a) $\dfrac{nw_s}{w} = \dfrac{1}{5}$; $w_s = 0.225$ inch; $\Phi = 2.75^{\circ}$.

Figure 9.- Static-pressure difference across the slots plotted against flow direction through the slots at $x = L$.

$nw_{s_X}/w = 0$ 1/8 w_s

Constant depth

θ_w | p_w/P_o

Variable depth | $\triangle p/P_o = (p_w - p_c)/P_o$

p_c/P_o

d_s

d_s

Constant depth along taper

Variable depth along taper

θ_w at end of slot taper, deg.

$\triangle p/P_o$ at end of slot taper

(b) $\dfrac{nw_s}{w} = \dfrac{1}{8}$; $w_s = 0.141$ inch; $\Phi = 2.75°$.

Figure 9.- Concluded.